Arc expression and protein-protein interactions in a mouse model of Alzheimer's disease

Exercise- and novelty-induced changes in Arc, BDNF, and PS1 expression and Arc PS1 interaction in APP/PS1 and WT mice

Johanne Eriksen Rimstad

This thesis is submitted in partial fulfilment of the requirements for the degree of Master in Biomedical Sciences

Department of Biomedicine
University of Bergen

Spring 2017

Acknowledgements

I would like to thank my supervisors Clive Bramham and Sudarshan Patil for their help in the process of completing this project.

Mouse brain tissue for the APP/PS1 vs. WT comparison studies was provided by the lab of Prof. Dr. rer. nat. Volkmar Lessmann.

Thanks also to the rest of the neuroscience research group; Hongyu, Lars, Marga, Maria, Oleksii, Sergei, and Tambu for always being prepared to help, and to my fellow Bramham students; Aina, Ida, Nils, Ram, and Sverre. A special thank you for the coffee breaks.

Last, but not least, a big thank you to my mom, for still pretending to be interested when I rant about technical issues.

Abstract

The overarching goal of this project was to help elucidate how some of the molecular mechanisms behind memory and learning differ between healthy brains and those with neurodegenerative diseases, specifically by studying changes involving the immediate early gene Arc, believed to be an essential regulator of synaptic plasticity. Expression of Arc protein, BDNF, and PS1 in the frontal cortex of APP/PS1 and WT mice housed in standard or enriched environments was compared using Western blotting. The results indicated that Arc expression did not differ significantly between the groups, BDNF expression was higher in mice housed in enriched environments, and PS1 expression was higher in the APP/PS1 mice, likely as a result of expressing a mutant PS1 protein in addition to the endogenous. Further, the project was concentrated on optimization of a co-immunoprecipitation protocol with the objective to study differences in the interaction between Arc and PS1 in APP/PS1 and WT mice. Application of the protocol to frontal cortex tissue from the two strains of mice housed in standard or enriched environments indicated no statistically significant difference in amount of immunoprecipitated Arc and PS1 among the groups of mice, moreover, results suggested that robust co-immunoprecipitation of PS1 with Arc or vice versa requires a continued optimization process.

Table of contents

List of abbreviations

Aβ	β-amyloid
AD	Alzheimer's disease
AICD	Amyloid precursor protein intracellular domain
AMPA	α-amino-3-hydroxy-5-methyl-4-isoxazolepropionate
AMPAR	α-amino-3-hydroxy-5-methyl-4-isoxazolepropionate receptor
ApoE	Apolipoprotein E
APH1	Anterior pharynx defective 1
APP	Amyloid precursor protein
Arc	Activity-regulated cytoskeleton-associated protein
Arg3.1	Activity-regulated gene 3.1
BCA	Bicinchoninic acid
BDNF	Brain-derived neurotrophic factor
BSA	Bovine serum albumin
CA	Cornu ammonis
CNS	Central nervous system
Cnx	Calnexin
Co-IP	Co-immunoprecipitation
CSF	Cerebrospinal fluid
DG	Dentate gyrus
Dnm2	Dynamin 2
Endo2	Endophilin 2
Endo3	Endophilin 3
FAD	Familial Alzheimer's disease
GST	Glutathione S-transferase
HD	Huntington's disease
HFS	High-frequency stimulation
IB	Immunoblotting
IgG	Immunoglobulin G
IP	Immunoprecipitation
KO	Knock-out
LTD	Long-term depression
LTP	Long-term potentiation
mRNA	Messenger RNA
ND	Neurodegenerative disease
NFT	Neurofibrillary tangle
NMDA	N-methyl-D-aspartate
NMDAR	N-methyl-D-aspartate receptor
PCR	Polymerase chain reaction
PD	Parkinson's disease
PEN2	Presenilin enhancer 2
PPI	Protein-protein interaction
PS1	Presenilin 1
PS1	Presenilin 2
SAD	Sporadic Alzheimer's disease
SDS	Sodium dodecyl sulfate
SDS-PAGE	Sodium dodecyl sulfate polyacrylamide gel electrophoresis
Stx4	Syntaxin 4

TREM2	Triggering receptor expressed on myeloid cells 2
TrkB	Tropomyosin receptor kinase B
WB	Western blot
WT	Wild-type

Summary

The world's population is ageing. With this comes an increase in age related diseases. Some threaten to send our bodies into rapid decline, such as cancer and heart disease; others, perhaps more terrifyingly, threaten to take away our mind, such as stroke or neurodegenerative diseases. The most common neurodegenerative disease is Alzheimer's disease (AD), characterized by progressive cognitive decline. Researchers are continuously working on developing drugs treat the disease, but so far, no cure has been found, and existing drugs only slow the progression for a while (Cummings et al., 2016).

One major reason treatments are so hard to develop is that the molecular mechanisms and drivers behind AD are still largely unknown. Traditionally, a short peptide called β-amyloid (Aβ) has been the prime suspect. When amyloid precursor protein (APP) is cleaved at a particular site, Aβ is produced and released into the space around neurons, where it aggregates and forms amyloid plaques, one of the hallmark features seen in post-mortem analysis of the brains of AD patients (Zhang et al., 2012a). The amyloid cascade hypothesis argues that overproduction or lack of clearance of these peptides and the subsequent formation of plaques drives the progression of the disease (Selkoe, 2002). Consequently, efforts have been focused on developing treatments to remove Aβ and amyloid plaques. However, as one anti-amyloid drug after the other fail to work, the amyloid cascade hypothesis is facing increasing levels of critique. While it is clear that amyloid plaque development is an important histopathological feature of AD, researchers are debating its functional role. Is it a causative factor, or rather a defense mechanism or result of another – unknown – cause; is it sufficient to remove plaques or does the Aβ peptide do its damage long before major aggregates are formed; and what role does spatial and temporal distribution of both peptides and plaques, as well as other pathological features of AD, play?

One of these other pathological features is synaptic failure (Selkoe, 2002; Serrano-Pozo et al., 2011). Synapses are the connections between neurons, the sites at which information is transferred from one cell to the next in the incredibly intricate network making up the central nervous system (CNS). Synapses are plastic structures, strengthened, weakened, and maintained with strict demand for appropriate regulation (Kuipers and Bramham, 2006). This plasticity is the basis for our ability to learn, form memories, and forget, and any disruption of the process will thus have major adverse consequences for brain function (Kuipers and Bramham, 2006). Loss and dysfunction of synapses may be a consequence of external factors such as amyloid plaques blocking connections to other neurons, of internal

factors such as defective regulatory processes within the cell or tau protein aggregation and destabilization of the cytoskeleton, or (perhaps most likely) a combination. Although much is still unknown, research is moving forward on several fronts in an effort to increase our understanding of the molecular causes, mechanisms, and consequences of AD. Here, I focus on synaptic plasticity in AD; specifically, whether the expression levels and protein-protein interactions of the regulatory protein Arc is altered in an animal model of the disease.

Chapter 1 gives the theoretical background for the project, starting with an introduction to AD and its pathology, followed by a general introduction to mechanisms of memory and learning, and synaptic plasticity in particular. I then introduce Arc, a protein thought to be responsible for regulation of synaptic plasticity, and discuss how Arc protein function may be related to formation of Aβ, thus raising the question of whether its function is disrupted in AD. From the theory, I deduce a set of testable hypotheses and discuss what methodological approach is best suited to test these. The concrete aims of the project are then summarized in chapter 2.

Methods and materials are described in Chapter 3. The material was mainly homogenized cortex tissue from a transgenic mouse model of AD, the APP/PS1 mouse, and the wild type (WT) mouse upon which the APP/PS1 is based (C57BL/6J). SDS-PAGE and Western blot (WB) was used to compare Arc, PS1, and BDNF protein expression in mice housed in different environments, as described in the results. Protein-protein interactions were studied with co-immunoprecipitation (co-IP) and GST-pulldown assays.

Chapter 4 contains the results, starting with the protein expression analyses. Next, the co-immunoprecipitation optimization process is described; a series of experiments were performed with variations in antibodies, lysis buffer, and the procedure, to achieve an effective protocol for mouse brain tissue. Results from co-immunoprecipitations carried out on APP/PS1 and WT mice are then presented, before the chapter is concluded with preliminary results from GST-pulldown assays performed on WT mice and rat tissue.

In chapter 5, I interpret the results and discuss whether they lend support to or debunk the hypotheses presented in chapter 1, and whether the aims of the project were reached. I also look closer at some limitations associated with the choice of materials and methods and how these affect the generalizability of the results, as well as limitations stemming from the initial theoretical assumptions of the project. The chapter is wrapped up with some thoughts on what the study has contributed to the field and where research on the topic could go from here.

1 Introduction

The last century has seen dramatic developments in medical science, and with that an increase in life expectancy, particularly in developed countries. However, though we are able to keep our bodies alive for longer, we are not yet able to stop them from declining. This poses a number of socio-economic as well as personal challenges, as people spend a smaller portion of their lives as tax payers and a larger portion in need of health care and economic support from their families and/or the government. Major efforts are thus being made in medical research to figure out how to efficiently treat – or better yet, prevent – age-related diseases. For many types of cancer, efficient treatments have been developed, and screening programs allow us to nip potential cases in the bud. Age-related neurodegenerative diseases, on the other hand, have proved particularly challenging, in large part due to the astonishing complexity of the human brain. Increasing our understanding of the brain, with its specialized actors and intricate networks, is thus critical in our effort to halt its decline. Neurodegeneration is a feature of several brain disorders, including Parkinson's disease and Huntington's disease, but most common, and arguably most infamous, is Alzheimer's disease.

1.1 Alzheimer's disease

1.1.1 Epidemiology and pathology

Alzheimer's disease (AD) is a neurodegenerative disease, characterized by cerebral atrophy and a progressive loss of cognitive function (Masters et al., 2015). It was first described in 1907 by German psychiatrist Alois Alzheimer, when he discovered substantial atrophy and extracellular plaques in the brain of his deceased patient Auguste Deter (Alzheimer, 1987). AD is the most common cause of dementia; it is thought to account for about 2/3 of all cases, amounting to 46.8 million cases worldwide, with the number estimated to reach 131.5 million by 2050 if no successful therapy is developed (Prince et al., 2015). The disease can be divided into early- and late-onset, the latter (>65 years of age) being by far the most common (Masters et al., 2015). Early-onset AD is typically the familial type (FAD), caused by recognizeable genetic mutations, while late-onset is predominantly sporadic (SAD) (Dorszewska et al., 2016). Both are, however, characterized by the same pathological manifestations in the brain. Patients typically develop atrophy of the hippocampus, entorhinal cortex, and cerebral cortex, areas crucial for memory formation and higher cognitive function (Figure 1.1) (Smith, 2002).

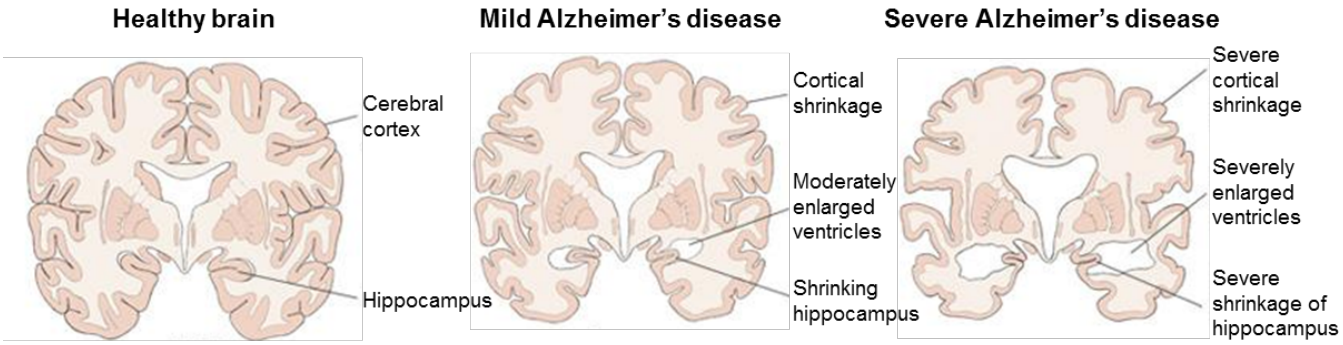

Figure 1.1 Progressive degeneration of the brain in Alzheimer's disease. Brain structures important for memory and higher cognitive function shrink in the brains of persons with Alzheimer's disease, notably the hippocampus and the cerebral cortex. Modified from Bob Morreale, BrightFocus Foundation.

In addition to a loss of neurons, brains from AD patients exhibit a loss of synapses and synaptic dysfunction in the same areas (Davies et al., 1987; Selkoe, 2002, 2008; Serrano-Pozo et al., 2011). Histologically, the disease is defined by two hallmark features: amyloid plaques composed of the short peptide β-amyloid (Aβ), and neurofibrillary tangles (NFTs) composed of tau protein (Figure 1.2) (De-Paula et al., 2012).

The pathology appears to progress through the brain according to a general sequence, with clinical symptoms developing correspondingly (De-Paula et al., 2012; Pearson et al., 1985; Smith, 2002). The rate of progression is variable and difficult to predict, but the disease can be divided into different phases. The first, and longest, is the preclinical stage, which may last for decades. In this phase, the patient does not present symptoms, although abnormal accumulation of Aβ can be detected with brain imaging (De-Paula et al., 2012; Masters et al., 2015). In the second, pre-dementia phase, the patient starts to show cognitive symptoms, including disorientation, loss of the ability to form and retain long-term memories, and problems with language and mood regulation. Pathology is typically evident in the entorhinal cortex, the hippocampus, and parts of the cerebral cortex (Braak and Braak, 1991; Thal et al., 2002). Later, it appears to spread through the cerebral cortex, corresponding to the loss of cognitive and physical function as the disease progresses (Smith, 2002). In the last, most severe stage, AD pathology reaches the cerebellum (Thal et al., 2002), which is responsible for motor control and coordination, and clinical symptoms include loss of bodily functions and ultimately death.

There is still no consensus on how or why the disease develops and progresses, but it is generally accepted to be in some way related to the formation of amyloid plaques and neurofibrillary tangles.

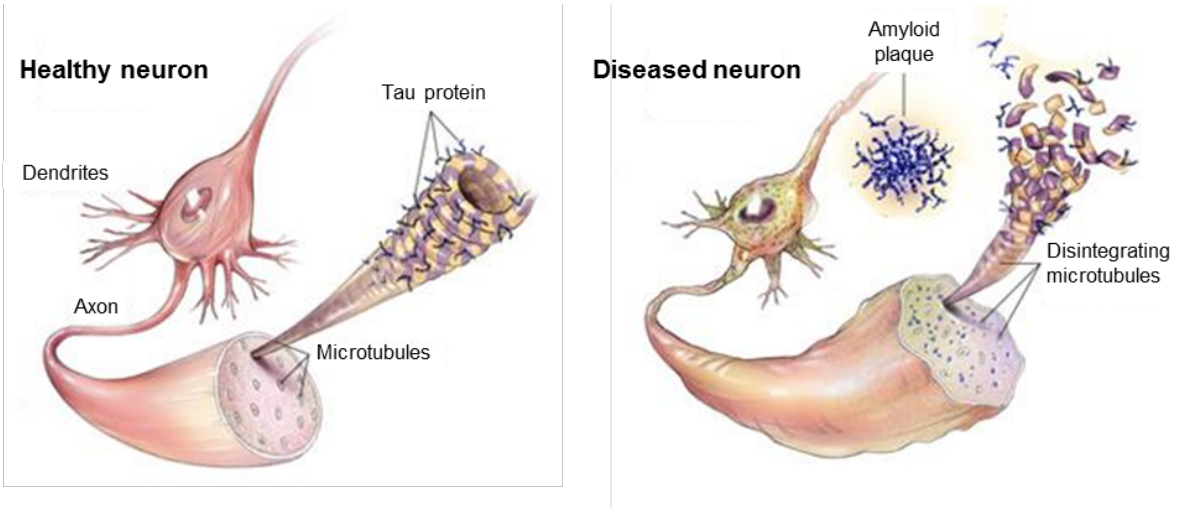

Figure 1.2 Protein aggregates in Alzheimer's disease. In healthy neurons, microtubules are stabilized by tau protein. In Alzheimer's disease, tau protein is hyperphosphorylated and dissociates from the microtubules, causing them to disintegrate and form neurofibrillary tangles inside the cell. In the extracellular space, Aβ peptides aggregate and form amyloid plaques. Modified from Bob Morreale, BrightFocus Foundation.

1.1.2 Aβ and amyloid plaques

Amyloid plaques are aggregates of Aβ, a peptide that has long been the prime suspect when it comes to AD pathogenesis. The amyloid cascade hypothesis argues that the main driver of AD is deposition of Aβ at one or more initial sites followed by spread and aggregation of Aβ oligomers, fibrils, and plaques throughout the brain, propagating synaptic failure and neuronal death as the cascade progresses, thus causing increasing loss of cognitive functions (Hardy and Higgins, 1992; Selkoe and Hardy, 2016).

Aβ is generated by proteolytic processing of the amyloid precursor protein (APP). APP is a type I transmembrane protein expressed in the brain, particularly at synapses, reported to play a role in promoting synaptic activity, dendritic spine formation, and neurite outgrowth (Hoe et al., 2012; Klevanski et al., 2015; Young-Pearse et al., 2008; Zheng and Koo, 2006). APP can function as a full-length protein, or it can enter into two main processing pathways, the non-amyloidogenic and the amyloidogenic (Figure 1.3) (Hoe et al., 2012). In the non-amyloidogenic pathway, APP is first cleaved extracellularly by the enzyme α-secretase, shedding the large soluble ectodomain sAPPα, then by the γ-secretase complex, yielding the small extracellular peptide p3 and the amyloid intracellular domain (AICD), shown to translocate to the nucleus and regulate gene transcription (Konietzko, 2012; Zhang et al., 2012a). In the amyloidogenic pathway, APP is cleaved by β-secretase (BACE1) instead of α-secretase, releasing sAPPβ. Subsequent cleavage by the γ-secretase complex yields AICD and Aβ, a peptide slightly longer than p3. This extra length makes Aβ sticky, increasing its

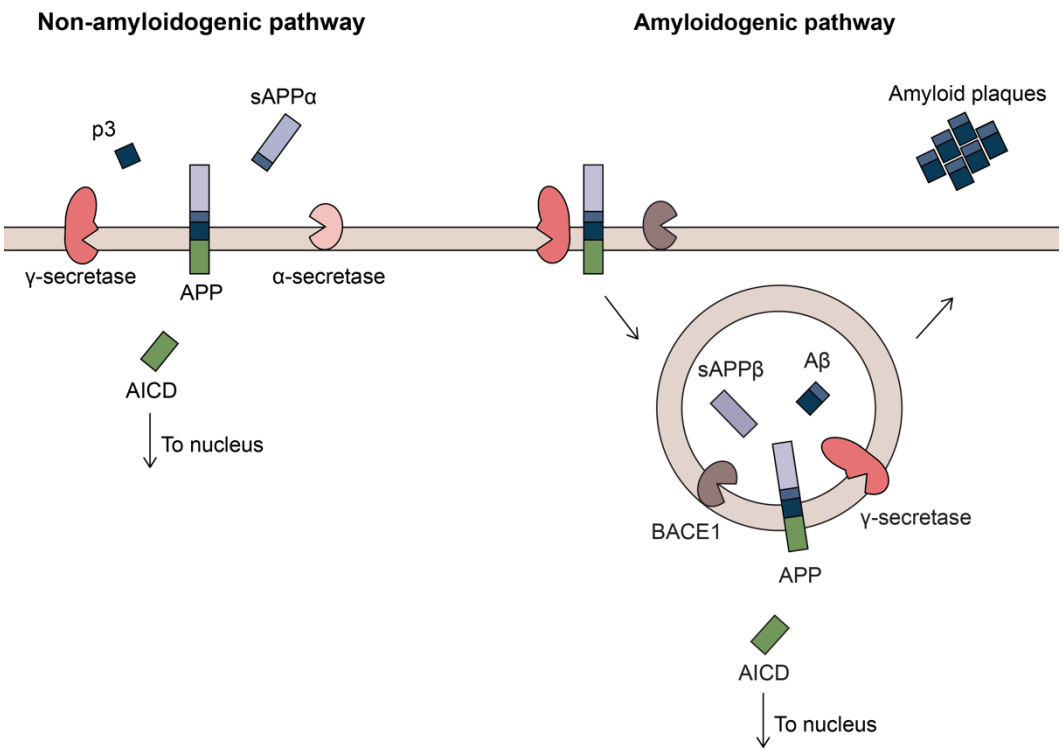

Figure 1.3 APP processing in the non-amyloidogenic and amyloidogenic pathways. In the non-amyloidogenic pathway, APP is cleaved sequentially by α-secretase and γ-secretase at the cell surface, yielding sAPPα, AICD, and the peptide p3. In the amyloidogenic pathway, APP is typically internalized with BACE1 and γ-secretase cleaved sequentially, yielding sAPPβ, AICD, and the peptide Aβ. Aβ tends to aggregate, resulting in extracellular amyloid plaques.

propensity to aggregate into oligomers which can clump together and form amyloid plaques (Zhang et al., 2012b).

Aβ aggregations like those in AD would, however, require that there is a substantial amount of Aβ present, as could result from increased APP processing and/or lack of clearance of Aβ. The former might be a consequence of overexpression of APP, or overactive processing enzymes. FAD is, indeed, correlated with multiple copies of the APP gene, or mutations in PSEN1 or PSEN2, genes encoding subunits of the γ-secretase complex (Dorszewska et al., 2016). Increased risk of SAD is associated with a specific allele of the gene encoding apolipoprotein E, which is implicated in reduced Aβ clearance; persons carrying the e4 allele of the ApoE gene have a higher risk of getting the disease, while the e2 allele seems to be a somewhat protective factor (Kim et al., 2009). Increased APP processing might also be a result of enhanced association of APP with the secretases. Whereas non-amyloidogenic processing appears to mainly happen at the cell surface, reports are that amyloidogenic APP processing typically occurs in endosomes; this, then, requires that APP, BACE1 and γ-secretase be

internalized and sorted into the same endosome, and dysregulation of this process could lead to overproduction of Aβ (Haass et al., 2012; Wu et al., 2011).

BACE1 processing is the first and rate limiting step in the amyloidogenic pathway (Haass et al., 2012). Its expression is elevated in AD patients, and drugs targeting BACE1 have been shown to reduce amyloid load in animal models (Evin and Hince, 2013). However, BACE1 knock-out (KO) mice do display some phenotypic abnormalities, suggesting that it may be difficult to develop drugs targeting BACE1 without adverse side effects (Zhang et al., 2012b). Moreover, as noted, the genes mutated in FAD encode subunits of the γ-secretase complex, indicating that understanding this complex is key both for elucidating mechanisms of AD pathogenesis and for drug development.

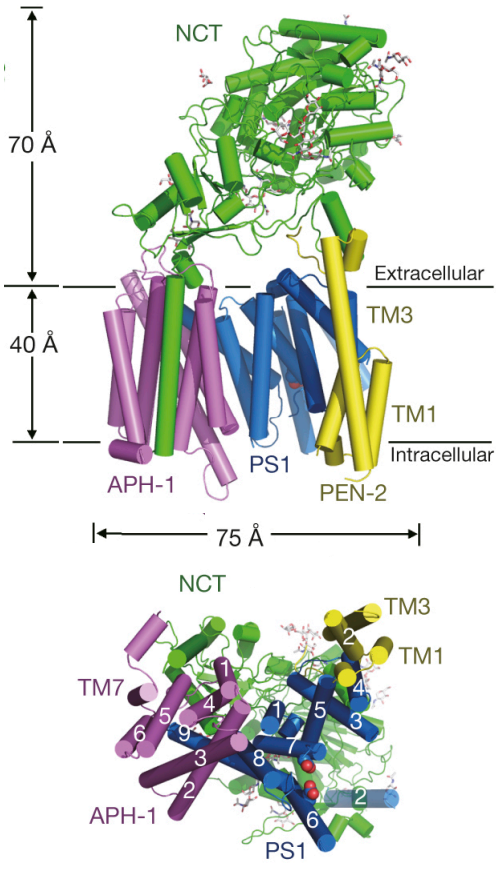

Figure 1.4 Structure of the γ-secretase complex. Structure of the γ-secretase complex consisting of presenilin 1, APH-1, PEN-2, and nicastrin (NCT). PS1 catalytic activity is dependent on two aspartate residues (red) on its transmembrane domains 6 and 7. Modified from Bai et al. (2015).

γ-secretase is a transmembrane protein complex composed of at least one presenilin (PS1/PS2), nicastrin, APH1, and PEN2 (Figure 1.4) (Bai et al., 2015; Fraering et al., 2004; Kimberly et al., 2003; Wolfe, 2006). Association of PS1 with PEN2 facilitates endoproteolytic cleavage of PS1 between transmembrane domains 6 and 7 (TM6 and TM7), yielding an N-terminal (NTF) and a C-terminal (CTF) fragment, which stay associated, forming an active heterodimer with two aspartate residues on TM6 and TM7 necessary for protease activity (Wolfe, 2006). A three-amino-acid motif on TM9 is thought to be involved in substrate recognition (Figure 1.5). In the case of the amyloidogenic pathway the substrate is APP, but γ-secretase is also involved in other cellular functions, most notably Notch signaling (Wolfe, 2006). γ-secretase does not, however, process APP in a single step or at a single site, but follows one of two stepwise processing lines yielding Aβ peptides of slightly different lengths (Haass et al., 2012). The last cleaving can occur after amino acid 37 to 43 of the Aβ domain, Aβ40 and Aβ42 being the most common products (Haass et al., 2012).

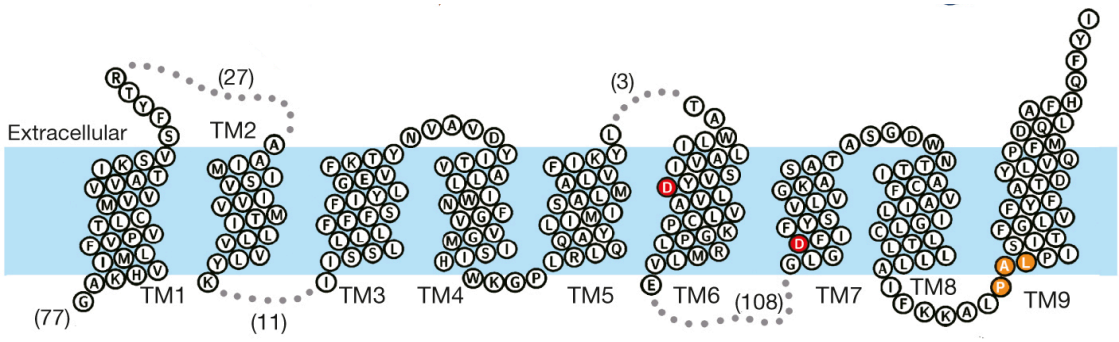

Figure 1.5 Presenilin 1 topology. Membrane topology diagram of presenilin 1, with its nine transmembrane domains. Aspartate residues necessary for catalytic activity in red, amino acids indicated in substrate recognition in orange. Figure from Bai et al. (2015).

Of these, Aβ40 is nine times more abundant in AD than Aβ42, yet amyloid plaques *in vivo* are mainly made up of the Aβ42 isoform, typically attributed to the extra Ile-Ala at its C-terminus making it more aggregation prone (Iljina et al., 2016). In line with this, an increase in the Aβ42/Aβ40 ratio is associated with increased plaque formation and neurotoxicity (Iljina et al., 2016). Importantly, the toxic effects of Aβ are manifest before they form solid plaques; Haass and Selkoe (2007) propose a model where amyloid plaques are reservoirs of soluble oligomers, the oligomers being the bioactive element causing synaptic dysfunction by associating to the neuronal plasma membrane at synapses, thus disrupting normal signaling events. Evidence of impaired synaptic structure and function in mouse hippocampal slices treated with Aβ oligomers supports this (Shankar et al., 2008). The composition of different Aβ isoforms in oligomers is difficult to determine in vivo, but modelling and in vitro studies suggest that even though Aβ42 is inherently stickier, Aβ40 and Aβ42 can readily co-oligomerize (Gu and Guo, 2013; Iljina et al., 2016). A preferential aggregation of Aβ42 with itself *in vivo* may therefore indicate that there are unknown *in vivo* mechanisms favoring this self-oligomerization (Gu and Guo, 2013).

Aβ oligomers may also function as seeds that are transmitted synaptically and promote aggregation, effectively being responsible for the cascade of amyloid pathology (Morales et al., 2015). Synapses and synaptic activity, then, could be important in AD pathology not only as victims, but as perpetrators, working as active transmitters of Aβ.

The question is posed, however, of whether Aβ generation is a causal factor in AD, or an effect following some other causal event. One intriguing proposition is that Aβ is not in fact a pathogen, but part of the immune system, protecting against infectious agents that have managed to cross the blood-brain barrier (BBB). In a recent study, Kumar et al. (2016) infected cell cultures, the nematode *C. elegans*, and mice with *Salmonella Typhimurium*, and found that elevated Aβ expression was indeed a protective factor, proposing a model where Aβ

inhibits the pathogens' ability to bind to the host cell, and eventually imprisons the pathogen by forming aggregates around it. Whether enhancement of Aβ in AD would be a result of a real or imagined infection remains to be resolved.

Another suggested physiological role for Aβ is that Aβ is part of a negative feedback mechanism normally functioning to mediate synaptic activity, that has somehow become too strong in AD (Kamenetz et al., 2003). Excess of one or more of the other products of amyloidogenic APP processing, sAPPβ and AICD, may also have harmful effects, as may a loss of function of products of the non-amyloidogenic pathway should APP be sequestered by β-secretase at the expense of α-secretase activity.

Other critics of the amyloid cascade hypothesis argue that focusing so heavily on Aβ is a mistake altogether, as tau protein pathology precedes amyloid plaque formation and correlates better with the progression of clinical symptoms (Duyckaerts, 2011).

1.1.3 Tau and neurofibrillary tangles

Neurofibrillary tangles (NFTs) are the second main histopathological feature of AD. NFTs are aggregations containing the protein tau, which normally functions to stabilize microtubules (Figure 1.2) (Wang and Mandelkow, 2016). Not as widely studied as Aβ, much is still not determined about why and how it is involved in pathogenesis and progression (Wang and Mandelkow, 2016). However, a common theory is that hyperphosphorylation of tau causes it to detach from the microtubules and form intracellular aggregates (Wang and Mandelkow, 2016). The aggregates appear to be toxic to the cell, and the lack of stabilizing tau protein causes microtubules to disintegrate, damaging the neuron and contributing to cell death (Wang and Mandelkow, 2016). Like Aβ pathology, propagation of tau pathology appears to occur through seeding, that is, a process where tau oligomers and protofibrils act as seeds that are transmitted synaptically and promote aggregation in a cascade-like manner (Walker et al., 2013). Also like Aβ pathology, tau hyperphosphorylation is hypothesized to be a defense mechanism rather than a cause of AD, a compensatory response triggered by oxidative stress (Lee et al., 2005).

In contrast to Aβ pathology, tau pathology development has been shown to correlate both spatially and temporally with the development of AD symptoms (Braak and Braak, 1991; Giannakopoulos et al., 2003). In fact, the different stages of tau pathology are used in AD diagnostics, referred to as Braak staging (Braak and Braak, 1991, 1997). Tau pathology is also a feature of other brain diseases, called tauopathies, including Huntington's disease (HD) (Wang and Mandelkow, 2016). This suggests that it might be a general cellular response to

different types of threats or perceived threats in the brain, and the increasing efforts into understanding tau physiology and pathology could reveal promising treatment options not only for AD, but for numerous other diseases, too.

1.1.4 More than tau and amyloid

In addition to the classical Aβ and tau aggregates, a wide range of potentially pathological factors have been identified in AD. Contributing factors may be increased levels of α-synuclein in cerebral spinal fluid (CSF) in AD (a peptide traditionally more associated with Parkinson's disease (PD)) (Majbour et al., 2017); dysfunction of the cholinergic system (Craig et al., 2011); mitochondrial dysfunction resulting in energy failure and oxidative stress (Onyango et al., 2016); vascular dysfunction leading to e.g. insufficient waste removal and supply of nutrients (Di Marco et al., 2015); or lack of plaque clearance by the glymphatic system (Xie et al., 2013). Glial cells are also implicated in AD pathogenesis. The most abundant glia of the central nervous system (CNS), astrocytes, provide vital support to neurons and the blood-brain barrier (BBB), but if damaged, they may contribute to increased Aβ plaque deposition through a vicious circle involving the inflammatory response (Avila-Muñoz and Arias, 2014). Microglia, the macrophage cells making up the brain's main immune response, appear to remove amyloid plaques by phagocytosis, but become activated and release inflammatory cytokines, resulting in a chronic inflammation state; a recent study found that knocking out a protein involved in recruiting microglia in an animal model of amyloidosis reduced damage to neurons, even though the plaque load was higher in the KO mice (Shi et al., 2017). In further support of the importance of the immune response in AD, certain genetic variants of the microglial surface receptor TREM2 are reportedly associated with a 2-4 fold increase in the risk of getting AD, almost as large as the effect of the ApoE e4 allele (De Strooper and Karran, 2016; Ulrich and Holtzman, 2016).

Given this range of involved factors in AD pathogeneses and progression, De Strooper and Karran (2016) argue that instead of focusing only on the two infamous proteins, a holistic approach is needed to understand the disease. They propose a three-stage model starting with a biochemical phase with unknown causes but characterized by Aβ and tau pathology, followed by a cellular phase where different types of brain cells respond to the stress of protein aggregation by developing compensatory mechanisms, and when these become irreversible, the disease transitions to a clinical phase of AD with manifest dementia.

Whatever the cause or causes, dysfunction, reduction, and loss of synapses is indisputably a consequence of Alzheimer's disease, particularly in the hippocampus and

neocortex (Scheff et al., 2006). Understanding why this leads to memory loss, and figuring out how it may be ameliorated, requires some understanding of normal memory function.

1.2 Mechanisms of memory

One of the most important functions of our brain is the ability to learn and form memories, allowing us to survive known dangers and adapt to new ones. Loss of this ability, e.g. by AD or traumatic injury, can be immensely debilitating. Not surprisingly, a central ambition in neuroscience is deciphering how the brain adapts in response to sensory inputs; how our experience of the world is translated into changes in the brain itself.

1.2.1 Localizing memory

Different brain regions are associated with different functions, and the regions most closely associated with the ability to form and retain long-term memories are the hippocampus and the neocortex (Squire et al., 2015). The neocortex is the outer layer of the vertebrate brain, and can be divided into the frontal, temporal, occipital, and parietal lobe; within these are different areas responsible for certain functions, such as speech, vision, olfaction, or executive function (Squire et al., 2013). The hippocampus is a subcortical brain structure located in the medial temporal lobe. It consists of the substructures Cornu Ammonis 1-3 (CA1-3) and the dentate gyrus (DG), and is functionally and anatomically connected to neocortical areas though the entorhinal cortex (Buzsáki, 1996; Neves et al., 2008; Rothschild et al., 2017). The hippocampus is essential to the process of memory consolidation, in which memories are transferred from short-term to long-term memory (Bartsch and Wulff, 2015). Sensory information is first received and processed in the neocortex, and then transferred to the hippocampus, which integrates the different inputs (e.g. relating the visual and olfactory inputs from a flower) (Squire et al., 2015). The hippocampus is then responsible for transferring the information back to the cortex for long-term storage through memory consolidation, resulting in a memory independent of the hippocampus (Eichenbaum, 2004). If the hippocampus is damaged and cannot perform its function in consolidating memories, a consequence will be loss of the ability to form new long-term memories such as can be seen in AD (Bartsch and Wulff, 2015).

Memory consolidation can be divided into systems consolidation and synaptic consolidation. Systems consolidation refers to the process of making the memory independent of the hippocampus, and appears to be dependent on accurately timed delivery of the brain-

derived neurotrophic factor BDNF to function properly (Bekinschtein et al., 2008). Synaptic consolidation refers to the protein synthesis dependent change in synaptic strength triggered by a pattern of repeated activation, and is part of what is called synaptic plasticity (Bramham, 2007).

1.2.2 Synaptic plasticity

The human brain is reported to contain approximately 86 billion neurons, which interact in networks through synapses (Azevedo et al., 2009). Neurons typically consist of one axon and multiple dendrites springing from a cell body (Squire et al., 2013). The axon connects to another neuron at a synapse, usually on a dendritic spine, where it can transmit signals (usually chemical, less commonly electrical) across a tiny cleft to the connecting neuron (Squire et al., 2013). Hebbian theory states that if one neuron signals, or fires, over a synapse and thus activates another neuron, the synapse will physically grow, strengthening the connection (Hebb, 1949). The current understanding of this mechanism is that specific firing patterns may induce strengthening, weakening, or stabilization of a connection. This dynamic and plastic nature of synapses is widely accepted to be the molecular basis for memory and learning, and is described using the concepts long-term potentiation (LTP), long-term depression (LTD), and homeostatic scaling (Squire et al., 2013).

LTP leads to strengthened synapses. In early phase LTP (E-LTP), high-frequency stimulation (HFS) of an excitatory glutamatergic neuron causes the insertion of α-amino-3-hydroxy-5-methyl-4-isoxazolepropionate receptors (AMPAR), stored in endosomal compartments, into the post-synaptic membrane. It also causes post-translational modification of existing AMPAR leading to increased conductance. In the late phase (L-LTP), which is dependent on brain derived neurotrophic factor (BDNF) signaling, more AMPAR are produced and inserted into the membrane, and the dendritic spine grows through remodeling of the actin cytoskeleton. This requires *de novo* protein translation and transcription, and is the same as synaptic consolidation. (Bramham, 2007; Bramham et al., 2010)

Strengthening connections between neurons is important for properly functioning memory and learning, but so is weakening and maintenance of strength. LTD leads to weakened synapses and shrinkage of dendritic spines. Induced by a pattern of low-frequency stimulation, LTD entails the removal of AMPAR from the postsynaptic membrane by endocytosis, and shrinkage of the dendritic spine. In homeostatic scaling, synaptic strength is stably maintained. (Bartsch and Wulff, 2015)

For normal functioning of memory and learning it is crucial that these processes be regulated in a highly specific and precise manner, allowing us to keep the information we do need and not waste capacity on that which we do not.

1.2.3 A regulator of synaptic plasticity

A protein that increasingly emerges as a candidate for the role of master regulator of synaptic plasticity is the activity-regulated cytoskeleton-associated protein, Arc/Arg.3.1 (Bramham et al., 2010; Shepherd and Bear, 2011). It is one of a group of genes termed immediate early genes (IEG), the name alluding to their rapid transcription as the primary response to inner or outer stimuli (Bahrami and Drabløs, 2016). Arc protein is mainly expressed in excitatory glutamatergic neurons in the hippocampus and neocortex, where it localizes to dendrites and the cell nucleus (Shepherd and Bear, 2011). Upon appropriate activation of an excitatory synapse, Arc is rapidly transcribed and mRNA delivered to dendrites for local translation (Bramham et al., 2010). The spatiotemporal precision of Arc protein synthesis and action relies on three features: 1) Docking of Arc mRNA to F-actin rich sites in dendritic spines, 2) rapid elimination of Arc mRNA via translation-dependent RNA decay, and 3) rapid degradation of Arc protein in ubiquitin proteasomal system (Bramham and Wells, 2007).

Arc protein is essential for memory consolidation (Plath et al., 2006), evidence supporting its involvement in regulation of both LTP, LTD, and homeostatic scaling (Bramham et al., 2008). It is hypothesized to distinguishing between these processes by operating as a multifunctional hub for other proteins, interacting with different sets of protein binding partners in the different processes (Bramham et al., 2010). In LTD, evidence indicates that Arc promotes internalization of AMPAR post-synaptically through interaction with proteins of the endocytic machinery dynamin 2 and endophilin 2 and 3 (Chowdhury et al., 2006). Arc also localizes to the nucleus, where it is implicated in homeostatic scaling through involvement in the transcriptional regulation of GluA1, a subunit of AMPARs, seemingly through interaction with promyelocytic leukemia (PML) nuclear bodies (Korb et al., 2013). Induction and consolidation of LTP has been shown to be Arc dependent (Messaoudi et al., 2007). A proposed model for this effector pathway is that HFS at a synapse triggers neuronal release of BDNF, which then binds to TrkB receptors at the post-synaptic membrane, thereby tagging the synapse for Arc mRNA as well as promoting transcription of Arc through the TrkB signaling pathway (Bramham and Messaoudi, 2005; Kuipers and Bramham, 2006; Soule et al., 2006). Enhanced Arc at the dendritic spine is then thought to regulate spine growth and remodeling of the actin cytoskeleton through direct binding to the actin-stabilizing protein

drebrin A and indirect binding to the actin filament severing protein cofilin (Nair et al., 2017). Arc also binds to the N-terminus of PS1, and given its known interaction with the endocytic machinery, it is proposed to be involved in endocytosis of APP and γ-secretase and their sorting into the same early endosome, where the amyloidogenic pathway takes place (Wu et al., 2011).

It is not yet established how the Arc response system is able to mediate and switch between these different effector pathways with very different outcomes. One possibility is that Arc associates with the particular sets of proteins as a result of post-translational modifications, conformational changes, or multimerization. Indeed, the protein appears to consist of two globular domains connected by a central unstructured hinge region, presumably allowing it to adopt different conformations, exemplified by an apparent change in structure upon binding PS1 (Myrum et al., 2015). Evidence also indicates that it is capable of self-oligomerizing, supporting a role for multimerization in regulating Arc's many functions (Myrum et al., 2015).

Whatever the mechanisms guiding Arc regulation of synaptic plasticity may be, the contrast between possible outcomes of Arc activity means it is crucial they not be disrupted.

1.3 Arc in Alzheimer's disease

Accumulating evidence for AD being a "synaptopathy", with synaptic dysfunction being a fundamental feature of the disease, suggests that Arc regulatory functions may be altered in affected brains (Kerrigan and Randall, 2013). This is supported by both genetic and biochemical studies into the relationship between Arc and AD.

One of these reports that soluble Aβ oligomers induces Arc expression in neurons (Lacor et al., 2004). Another demonstrates that Arc is necessary for the activity-dependent generation of Aβ (Wu et al., 2011). Taken together, this implies that there may be a positive feedback mechanism involved, which under pathological conditions could lead to propagation of Aβ production (Guntupalli et al., 2016). The mechanisms by which Arc influences AD pathology is likely to involve dysregulation of AMPAR trafficking, a theory that is supported by experimental evidence (Hsieh et al., 2006; Palop and Mucke, 2010; Wu et al., 2011). Increased AMPAR endocytosis resulting from increased Arc LTD activity would likely contribute to disruption of neural signaling networks, which could in turn play a part in propagation of pathology.

Genetic studies have also reported a connection between Arc and AD. A study on a Swedish cohort reports finding a variant of the ARC gene that reduces the risk of AD (Landgren et al., 2012); another has revealed variants of ARC associated with AD risk in Han Chinese, likely by either altering protein structure or increasing transcription of Arc mRNA (Bi et al., 2017). Mutations in the ARC gene is also implicated in schizophrenia, reinforcing the notion that disrupted Arc activity can severely interfere with normal brain function (Fromer et al., 2014; Huentelman et al., 2015; Purcell et al., 2014).

Altered expression levels of Arc appears to influence AD pathology, as supported by findings that AD patients are reported to overexpress Arc (Kerrigan and Randall, 2013). However, this alteration in expression levels appears to not be uniform; Rudinskiy et al. (2012) studied Arc expression in response to a visual stimulus and found that fewer neurons close to amyloid plaques express Arc, but those that do, overexpress. This complex expression pattern may explain that some studies indicate increased Arc activity in AD while others indicate decreased (Kerrigan and Randall, 2013). A study on the amygdala and hippocampus of a transgenic mouse model of AD found that soluble Aβ was reduced with long-term exercise, likely as a result of increased activation of the BDNF-TrkB pathway and Aβ clearance (Lin et al., 2015). Part of the effect of activating the BDNF-TrkB pathway appears to come from activation of Arc (Bramham and Messaoudi, 2005), indicating that Arc expression may be a relevant factor in this increased clearance. In a study on a transgenic mouse model of amyloidosis, Arc mRNA was found to be present at lower levels than in wild type (WT) mice, and novelty exposure did not increase Arc mRNA as much in the transgenic mice as in the WT (Christensen et al., 2013), supporting the idea that the expression level of Arc protein is disrupted in AD. This expectation can be expressed as two concrete hypotheses:

H1 Arc protein expression in the brain before external stimulus < Arc protein expression in the brain after external stimulus

H2 Stimulus-induced change in Arc protein expression in healthy individuals > stimulus-induced change in Arc expression in individuals with AD

Disrupted Arc function may stem from a disrupted expression level, or from alterations in its ability to interact with the right proteins at the right time. As described, Arc is known to interact with several proteins of the endocytic machinery to internalize AMPAR, and is demonstrated to bind directly to PS1 of the γ-secretase complex. A feasible model could thus

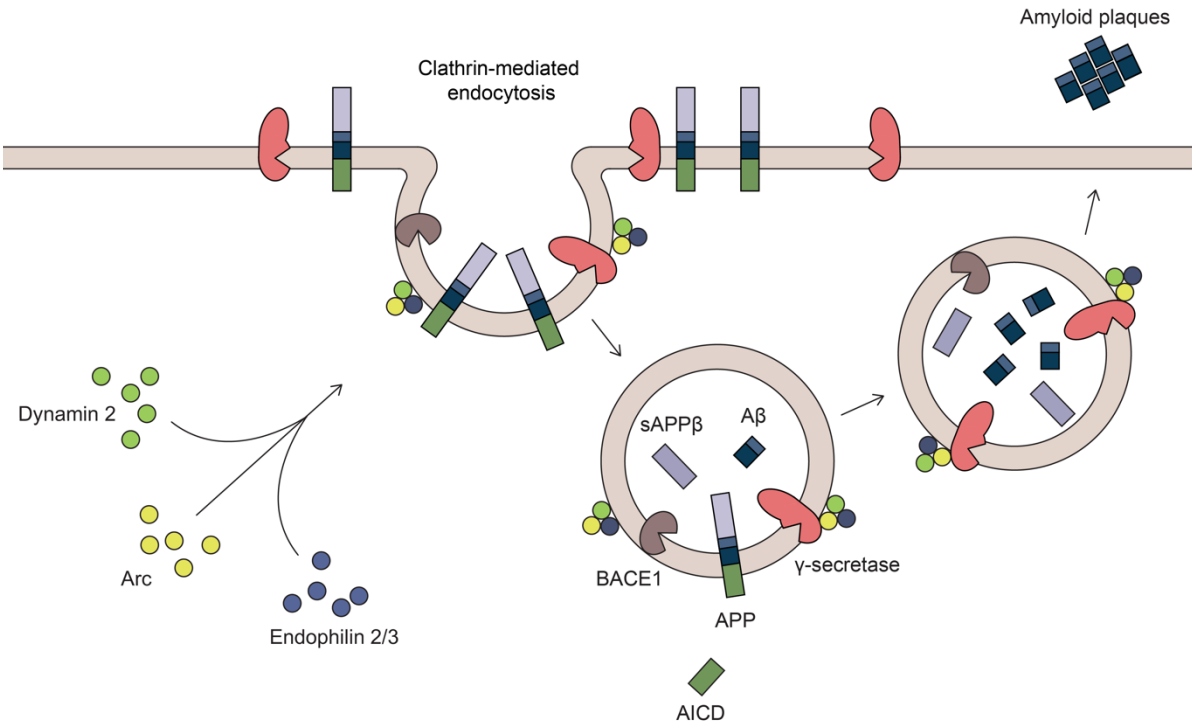

Figure 1.6 Proposed model of Arc regulating sorting of APP and γ-secretase in early endosomes. Arc interacts with dynamin 2 and endophilin 2/3 in the endocytic machinery to regulate endocytosis (Chowdhury et al., 2006), and enhances association of APP with gamma secretase in early endosomes through direct interaction with PS1 (Wu et al., 2011). Adapted from Wu et al. (2011) and Bali et al. (2010).

be that a physiological function of Arc is to regulate endocytosis of APP, BACE1, and/or γ-secretase through cooperation with dynamin 2 and endophilin 2/3, and to promote sorting of APP, BACE1, and γ-secretase into the same early endosome through its direct binding to PS1, thereby facilitating the production of Aβ (Figure 1.6) (Wu et al., 2011). Dysregulation of such a process could lead to overproduction of Aβ. In accordance with this, Arc has been reported to be necessary for activity-dependent increase in Aβ by enhancing the association of APP with BACE1 and γ-secretase in early endosomes, though basal levels of Aβ were apparently not influenced by knocking out Arc (Wu et al., 2011). In sum, interaction between Arc and the γ-secretase complex is expected to be a physiological function, but Arc activity in this pathway leading to Aβ generation is expected to be higher in AD brains. Changes in Arc function as regulator of this process can be studied, concretely, as changes in protein-protein interactions. We may thus deduce the experimentally testable claim:

H3 Arc/PS1 interaction in healthy brains < Arc/PS1 interaction in AD brains

Answering these hypotheses requires a set of materials and methods appropriate for the task.

1.4 Methodology

The present project was part of a collaboration with other labs across Europe investigating a proposed link between BDNF-TrkB signaling and neurodegenerative diseases (CircProt). This entailed some restrictions on the materials and methods available for this project, to allow its integration with other branches of the overarching project.

1.4.1 Choice of materials

The different work packages of the CircProt project are set to focus on different things, e.g. behavioral studies comparing the effect of different genes and environments on the behavioral phenotype. Later stages of the present project will introduce electrophysiology as a method to investigate the effect of AD pathology on LTP induction. These kind of studies favor the use of an animal model as material, as opposed to patient-derived material or cell cultures. The ambition to integrate this study in the overarching project made animal tissue the preferred choice of material for this part of the project, too. The animal model chosen was APP/PS1 mice, a transgenic strain of mice expressing APP and PS1 with mutations associated with FAD. It is chiefly a model of amyloidosis and only to a lesser degree includes tau pathology. By definition, then, it does not capture all aspects of AD. This may be seen as a weakness, as it makes it less valid to infer that what occurs in the model occurs in human patients, but it also has strengths in that it reduces the number of variables and allows a targeted study of particular aspects of the disease.

Answering H1 and H2 required the controlled introduction of a stimulus and subsequent analysis of Arc expression. This was done reliably in an animal model by introducing physical exercise in the form of a running wheel. However, the presence of a running wheel is enrichment of the mice's environment and a stimulus in itself in the form of an introduced novelty, which may in itself have an effect on protein expression. To distinguish between these two potential effects, a test group housed with a "non-running", or dummy, wheel was included.

All hypotheses could be studied with biochemical analyses of the brains of the model mice. Homogenized tissue lysate from the frontal cortex was chosen as the material, as amyloidosis is reported to appear here early and reliably in AD (as described above). Lysed tissue from whole cortical regions is, however, material providing relatively low resolution. In addition to neurons, the lysate will include astrocytes, microglia, and blood cells, among other things. While H1 and H2 are best studied using an animal model, H3 might have been

studied using neuronal cell cultures or combined cultures, thereby lowering the number of variables. On the other hand, *in vivo* studies on animal models is arguably closer to the physiological reality in humans than *in vitro* studies, and the introduction of some variables (e.g. the vascular and glymphatic system) may be a strength rather than a weakness; tissue lysate was therefore chosen as the material for this section of the study, too.

1.4.2 Choice of methods and proteins of interest

For the studies of Arc expression levels (H1 and H2), Western blotting was judged an appropriate method. Arc, BDNF, and PS1 were chosen as proteins of interest; Arc because it is the central element of the hypotheses, BDNF because of its involvement in synaptic plasticity and activity-induced release (as described above), and PS1 because of its role as a link between Arc and AD pathology.

Arc does not appear to have inherent catalytic activity; rather, as discussed, it can be seen as a multifunctional hub, or adapter protein, working through interactions with other proteins, coordinating their actions and localization. Arc function can thus be assessed with protein-protein interaction (PPI) methods. Co-immunoprecipitation allows study of interactions between proteins in their native form, and was therefore selected as the main method for studying Arc/PS1 interaction. To control for the possibility that findings were an artefact of the method, the ambition was to use GST-Arc pulldown assay, though this part of the project was not carried out to completion. In an effort to answer H3, co-immunoprecipitation was carried out with Arc and PS1 as “bait” and “prey”, alternately. The methods needed optimization before being judged valid and reliable; other known and suspected Arc interaction partners (calnexin, dynamin 2, PSD-95, syntaxin 4) were used for that purpose.

2 Aims

The present research project is part of the JPND supported collaboration CircProt, and the overarching aim was to carry out preliminary biochemical analyses of Arc protein expression and the Arc interactome in APP/PS1 mice.

Specifically, the first aim was to compare Arc, BDNF, and PS1 expression in APP/PS1 and WT mice, assess whether enrichment of the environment influences the expression of these proteins, and if so, whether it has a different effect in APP/PS1 mice than in their WT littermates. The second was to develop effective co-immunoprecipitation and GST-Arc pulldown protocols for elucidating differences in the Arc protein interactome in mice, and to utilize these to compare Arc protein interactions in APP/PS1 and WT mice, focusing on changes in Arc/PS1 interaction as an indication for changes in Arc regulated trafficking of the γ-secretase complex.

3 Materials and methods

3.1 Animals

The study was carried out in accordance with Norwegian regulations on the use of animals in experiments. For the experiments comparing WT, AD model mice, and different housing options, mouse tissue from AD model mice were received from the lab of Prof. Dr. rer. nat. Volkmar Lessmann, Otto-von-Guericke-University Magdeburg, Germany. Samples were frontal cortex tissue from male APP/PS1 mice and their WT littermates, kept in standard housing, with two groups having either a running wheel or dummy wheel (not spinning) introduced at 5th month after birth, then kept in the cages for 2 months before dissection. APP/PS1 is a transgenic mouse model of amyloidosis developed by the lab of Prof. Dr. Mathias Jucker (Radde et al., 2006), created on a C57BL/6J background. The strain expresses a chimeric mouse/human APP gene containing the "Swedish mutation" (Mullan et al., 1992) and PSEN1 containing an L166P mutation, both controlled by the Thy1 promoter, allowing the production of human Aβ, preferentially Aβ42. Amyloid plaques appear first in the neocortex at 6-8 weeks and in the hippocampus at 4 months; impaired LTP between 6 and 8 months (Gengler et al., 2010). C57BL/6J mice used in the optimization process were handled by the Laboratory Animal Facility staff at the Faculty of Medicine and Dentistry at the University of Bergen, in accordance with The animal welfare act and The regulation on the use of animals in research. For this set of experiments, whole cortex was collected from 2-3 months old animals.

3.2 Antibodies

The following antibodies were used for western blotting and immunoprecipitation, as described in the results section: mouse anti-Arc monoclonal (C7; Santa Cruz sc-17839); rabbit anti-Arc polyclonal (H300; Santa Cruz sc-15325); rabbit anti-Arc polyclonal (Synaptic Systems 156003); guinea pig anti-Arc polyclonal (Synaptic Systems 156005); rabbit anti-PS1 monoclonal (Abcam E2000Y); mouse anti-PS1 monoclonal (Abcam ab-15456); rabbit anti-PS1 polyclonal (Sigma P7854); rabbit anti-calnexin C-term polyclonal (Enzo Life Sciences ADI-SPA-865); goat anti-calnexin polyclonal (C-20; Santa Cruz); mouse anti-GAPDH monoclonal (6C5; Santa Cruz sc-32233) rabbit anti-BDNF polyclonal (N-20; Santa Cruz sc-546); mouse anti-syntaxin 4 monoclonal (Abcam ab-77037); rabbit anti-syntaxin 4

monoclonal (EPR15473; Abcam ab-184545); goat anti-dynamin 2 (C-18; Santa Cruz sc-6400); rabbit anti-dynamin 2 polyclonal (Merck ABT49); normal mouse IgG (sc-2025), normal rabbit IgG (sc-2027), normal goat IgG (sc-2028) (all from Santa Cruz); goat anti-rabbit IgG horseradish peroxidase (HRP) conjugated H+L chain specific (401315); rabbit anti-goat IgG-HRP H+L (401515); goat anti-mouse IgG-HRP H+L (401253) (all from Calbiochem); goat anti-guinea pig IgG-HRP, H+L (Southern Blot Biotech 6090-05); goat anti-rabbit IgG-HRP (sc-2030), goat anti-mouse IgG-HRP (sc-2055), rabbit anti-goat IgG-HRP (sc-2768) (all from Santa Cruz). Primary WB antibodies were prepared in 5% BSA in 1X Tris-buffered saline (TBS) with 0.1% Tween 20 (TBST), secondary antibodies in 1X TBST.

3.3 Sample preparation

Samples were homogenized in 400-500 µL lysis buffer (20 mM HEPES pH 7.4, 137 mM NaCl (unless otherwise stated), 0.5% Nonidet P-40, 1 mM EDTA, 5% glycerol, 1 mM NaF (unless otherwise stated), 1 mM Na_3VO_4, cOmplete Mini protease inhibitor cocktail tablet (Roche)) and centrifuged at 13,000 rpm, 4℃ for 10 minutes. The supernatant was collected and protein concentration determined by BCA assay (Pierce BCA Protein Assay Kit) using a VersaMax microplate reader and SoftMax Pro software (v. 4.7.1).

3.4 Protein expression analysis

Lysate containing 40 µg protein were incubated with 1:1 Laemmli sample buffer for 5 minutes at 95℃, then subjected to SDS-PAGE and Western blotting.

3.5 Co-immunoprecipitation

The following procedure was used in the protocol optimization experiments, with variations as noted in the results section. Protein G-sepharose 4 Fast Flow beads (GE Healthcare) were washed 3X in 1X PBS. 2 µg IgG antibody against the protein to be immunoprecipitated or purified IgG from the same species as the antibody was incubated with 20 µL washed beads and lysis buffer to 500 µL, rotating for 1 hour at room temperature (RT) (unless otherwise stated). After incubation with antibody, beads were washed 1X in 1X phosphate-buffered saline (PBS). Lysate containing 250 µg (hippocampus) or 300 µg (cortex) protein and lysis buffer to a total volume of 500 µL was added, and incubated rotating for 2 hours at 4℃ (unless

otherwise stated). Beads were then gently washed 3X in lysis buffer at 4℃. Proteins were eluted from beads and denatured by incubating for 5 minutes at 95℃ with 1:1 Laemmli sample buffer (Bio-Rad) (unless otherwise stated), before separation by SDS-PAGE. Lysate inputs containing 40 µg protein were denatured the same way.

For the co-immunoprecipitations comparing APP/PS1 mice and their WT littermates, antibody was not pre-bound to beads; 20 µL beads, 2 µg antibody and lysate from frontal cortex (300 µg protein) were incubated with lysis buffer up to 500 µL overnight at 4℃.

3.6 Bacterial transformation and protein purification

80 µL of B21 competent cells were thawed on ice and incubated with 50-100 ng of PCR product (GST plasmids or GST-Arc plasmids) for 15 minutes on ice, then subjected to heat pulse at 42℃ for 90 seconds in a water bath. Tubes were put back on ice and 500 µL LB broth (200 µg LB in 100 mL water) was added to each, followed by 1 hour incubation at 37℃. Agar medium was prepared from 100 mL water, 2 g LB broth and 1.5 g agar, boiled in microwave and cooled to ~50C, then added 50 µL of 100mg/mL Ampicillin (1:1000), and distributed onto petri dishes (~25 mL/dish). Transformed bacteria were plated and incubated overnight at 37℃. Cultures were prepared from single bacterial colonies incubated in LB broth medium for 3 hours at 30℃, shaking at 250 rpm, then cooled to 10-13℃ while still shaking, then added 1 mM isopropylthiogalactoside (IPTG) and incubated overnight at 10℃, 250 rpm, to an OD of 0.5-1.5 at 600 nm. The cultures were centrifuged at 8000 rpm for 7 minutes and the supernatant discarded. Pellets were resuspended in STE buffer (100 mM NaCl, 10 mM Tris-HCl pH 8.0, 1 mM EDTA), then 10 mM DTT was added and the samples sonicated 3x30s with 30s intervals. 1% Triton X-100 was added before incubation for 30 minutes at 4℃. Lysate was centrifuged 13,000 rpm, 4℃ for 30 minutes and the supernatant incubated with washed glutathione sepharose beads (GE Healthcare) for 2 hours at 4℃. Bead mixture was passed through a filter column and the column washed 4x with STE buffer with 1% Triton X-100, 4x with 50 mM Tris-HCl pH 8.0, and the proteins eluted with 3x5 minutes incubation with 10 mM L-Glutathione in 50 mM Tris-HCl pH 8.0.

3.7 GST pulldown

20 µL glutathione sepharose beads (GE Healthcare) were incubated with 10 µg purified protein (GST or GST-Arc) for 2 hours at 4℃, then 1 mL 5% filtered BSA was added followed by overnight incubation at 4℃. The next day, the supernatant was removed and beads were washed once in 1X PBS and incubated with 300 µg lysate for 2 hours at 4℃. Beads were washed 3x with 1X PBS and the proteins eluted with 1:1 Laemmli sample buffer (Bio-Rad) with 5% β-mercaptoethanol, incubated for 5 minutes at 96℃, and separated by SDS-PAGE.

3.8 SDS-PAGE

5 µL PageRuler was used as the protein standard for all gels. Samples were loaded onto 8% or 10% SDS-PAGE gels (as described in results section) and run on 100V for ~1.5 hours in 1X TGS buffer.

3.9 Western blotting

Proteins were transferred from polyacrylamide gels to nitrocellulose membranes using a Bio-Rad Trans-Blot Turbo machine and the StandardSD program (25V, 1.0A, 30 min). Membranes were then blocked in 5% dry milk for 1 hour at RT, rinsed 1X in 1X TBST, and incubated with primary antibody (1:1000 in 1X TBST with 5% BSA) overnight at 4℃. The next day, membranes were washed 3X5 minutes in 1X TBST and incubated with secondary antibody for 1 hour (1:5000 in 1X TBST for antibodies from Santa Cruz; 1:10,000 in 1X TBST for antibodies from Calbiochem and Southern blot biotech), then washed 3X5 minutes in 1X TBST. Blots were visualized with enhanced chemiluminescence (Pierce ECL Western Blotting Substrate), using a BioRad ChemiDoc molecular imager and Quantity One 4.6.6 software.

After imaging, membranes were stripped of antibodies by incubation with stripping buffer (62.5 mM Tris-HCl pH 6.8, 2% SDS, 0.8% β-mercaptoethanol) for 45 minutes at 50℃, then rinsed 3X in ddH_2O, washed 3X5 minutes in 1X TBST, blocked in 5% dry milk for 1 hour at RT, rinsed 1X in 1X TBST, and reprobed with a different antibody.

3.10 Blot quantification and statistics

Western blots of Arc, BDNF, and PS1 in the APP/PS1 and WT lysate were quantified in ImageJ, and normalized to GAPDH. For each protein, values were normalized to WT mice in standard housing. Western blots from Arc and PS1 immunoprecipitation experiments comparing APP/PS1 and WT mice were quantified with the same method and normalized; when blotting for the same protein as immunoprecipitated, values were normalized to the value representing the WT mouse housed in standard cages (e.g. amount of Arc IP-ed from mice with a running wheel per amount of Arc IP-ed from mice in standard housing); when blotting for that of the two proteins not immunoprecipitated, values were normalized to the corresponding value for the immunoprecipitated protein (e.g. amount of PS1 in the Arc IP per amount of Arc in the Arc IP). Two-way ANOVA with Holm-Sidak's multiple conparisons test were carried out in Prism 7.

4 Results

Two main sets of experiments were performed to (1) study how expression of Arc, BDNF, and PS1 is influenced by different housing options in APP/PS1 and WT mice, and (2) compare the interaction between Arc and PS1 in APP/PS1 and WT mice. To carry out the latter, a methods optimization process was necessary.

4.1 Changes in Arc, BDNF, and PS1 expression

Western blots of Arc, BDNF, and PS1 were performed on frontal cortex tissue lysate from 7 months old male APP/PS1 mice (AD model) and their WT littermates, housed in three different conditions: standard housing, with a running wheel introduced 5 months after birth, or with a "non-running", or dummy, wheel introduced 5 months after birth (Arc: n=5; BDNF: n=4; PS1: n=5). Representative blots are shown in Figure 4.1. Probing with antibody against Arc gave bands at ~55 kDa, corresponding to Arc protein size. Across the 5 experiments, the variation in intensity of the bands in different lanes did not appear to follow a specific pattern. Probing with antibody against BDNF gave protein bands at ~25 kDa, corresponding to expected BDNF size, and the intensity of the bands appear to be lower in lanes loaded with samples from mice housed in standard conditions, than the other groups. Probing with anti-PS1 gave one band at ~18-19 kDa in the lanes loaded with WT samples, corresponding to expected size for the C-terminal fraction of PS1, whereas in the lanes with APP/PS1 samples, an additional band of roughly the same intensity was detected just above the first.

5 repetitions (4 in the case of BDNF) of Western blots were quantified and normalized to the housekeeping gene GAPDH to control for differences in protein concentration due to variation in the amount of sample loaded. In quantification of PS1, both bands detected at ~18-19 kDa were included. For each protein, means of the normalized values from the six groups

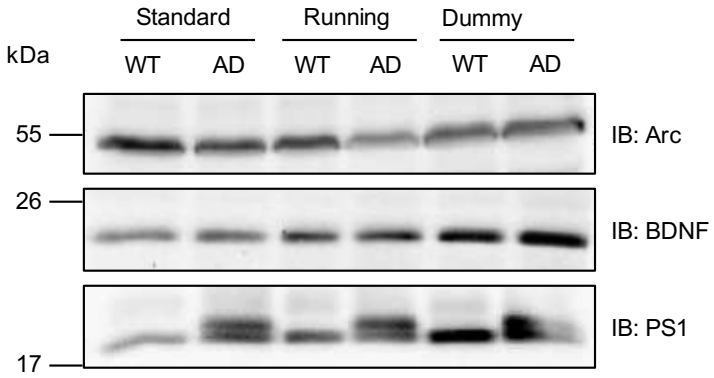

Figure 4.1 Representative Western blots from protein expression analyses. Western blotting of Arc, BDNF, and PS1 in frontal cortex of WT and APP/PS1 (AD) mice kept in standard housing, with running wheel, or with a dummy wheel. Blots were also probed with GAPDH for loading control (not shown).

of mice (two strains and three housing options) were normalized to the value for the given protein in WT mice housed in standard conditions, and plotted in histograms, error bars representing SEM (Figure 4.2). Two-way ANOVA with multiple comparisons (Holm-Sidak) was performed for each protein, with comparisons done (1) between different mouse strains housed together and (2) between groups of one mouse strain housed differently. No significant change in Arc expression was found with either varying mouse strain or housing. BDNF expression in the WT groups housed with a running or a dummy wheel was higher than in WT mice housed in standard conditions, both differences statistically significant and of similar magnitude. No significant difference in BDNF expression was detected between the two strains of mice. For the groups housed in standard cages and with a running wheel, PS1 expression was found to be significantly higher in APP/PS1 mice than in WT mice, with a larger and more statistically robust difference in the standard housing group. No statistically significant difference in PS1 expression was detectable between the groups

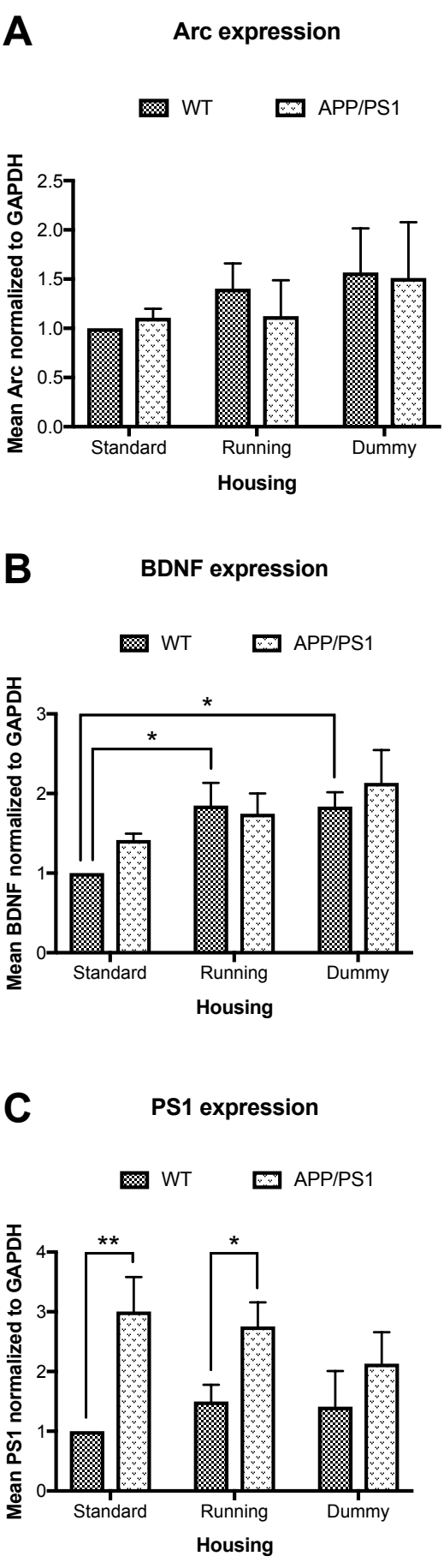

Figure 4.3 Mean Arc, BDNF, and PS1 protein expression in WT and APP/PS1 mice housed in different conditions. Mean normalized (GAPDH) expression of Arc (n=5), BDNF (n=4), and PS1 (n=5), quantified from Western blots. In each plot, columns are normalized to the column representing WT standard housing mice. Both bands detected at ~18-19 kDa in PS1 blots were included in quantification. Two-way ANOVA with multiple comparisons was performed, comparisons done (1) between different mouse strains housed together and (2) between groups of one mouse strain housed differently. Error bars: standard error of the mean (SEM). * $p < 0.0332$, ** $p < 0.0021$

housed in different conditions or between the two strains in the group housed with a dummy wheel.

4.2 Optimization of co-immunoprecipitation protocol

Comparing the strength of interaction between Arc and PS1 in the two strains of mice using co-immunoprecipitation required development of an optimized protocol. An effective protocol demonstrated to co-immunoprecipitate Arc and several known binding partners from rat tissue was previously established by the lab (see appendix 1), but as the physiology of mice is not identical to that of rats, the protocol could not be expected to be directly transferrable to a different species without adjusting a number of reagents and parameters. The established rat protocol was used as the basis for co-immunoprecipitation in mouse tissue, then adjusted through a series of experiments varying antibodies, buffers, and procedure. Lysed WT mouse cortex was used for all experiments.

4.2.1 Selecting antibodies for immunoprecipitation and immunoblotting

Effective antibodies are fundamental to a functioning co-immunoprecipitation, thus the optimization process began with a set of experiments comparing the efficacy of different antibodies in both immunoprecipitation and immunoblotting. Co-immunoprecipitations were carried out using three different antibodies for Arc; monoclonal anti-Arc C7 and polyclonal anti-Arc H300 from Santa Cruz biotech, and polyclonal anti-Arc from Synaptic systems; to determine which was the most effective in immunoprecipitating Arc (Figure 4.3 A). Probing membranes for Arc yielded bands at ~55 kDa, the expected size for Arc, in all three lanes containing immunoprecipitation samples, but the strongest contrast to the IgG control was seen in the lane where anti-Arc C7 was used.

For PS1 immunoprecipitation, it was decided that an antibody raised against an epitope on the N-terminus of the protein was the best option, as that is where Arc is shown to bind and PS1 undergoes endoproteolysis yielding C-terminal and N-terminal domains that might dissociate during the co-immunoprecipitation process. Because of a limited selection of commercially available antibodies, monoclonal anti-PS1 from Abcam was the only feasible choice.

After selecting anti-Arc C7 for co-immunoprecipitation, a series of Arc immunoprecipitations were carried out and immunoblotted with a selection of anti-Arc primary antibodies (Figure 4.3 B). C7 is produced in mice, thus rabbit and guinea pig derived

antibodies were tested, but not mouse, to avoid non-specific binding of the primary antibody to the C7 IgGs. Both anti-Arc derived from guinea pig and rabbit from Synaptic systems (SS) gave strong signals at around ~55 kDa; anti-Arc from Santa Cruz biotech (SC) also yielded a signal at the expected size for Arc, but a weaker one. Probing with rabbit anti-Arc from Synaptic systems yielded a band at ~50 kDa which was not seen in the lysate, corresponding to the size of IgG heavy chains.

Three different primary antibodies against PS1 were tested on lysate to assess their effectiveness and efficiency in recognizing PS1 (Figure 4.3 C). Mouse-derived monoclonal anti-PS1 was expected to yield a band at 28 kDa band, corresponding to the PS1 N-terminus, but no band was detected at that site. Probing with monoclonal rabbit anti-PS1, targeting the C-terminus, gave bands at both around 19 and 26 kDa, the first of which was expected, the second of which might corresponds to the size of the IgG light chain or the PS1 N-terminus. The third antibody tested, polyclonal rabbit anti-PS1, also gave signals at the expected 19 and the unexpected 26 kDa, but these were much weaker than those in the monoclonal rabbit anti-

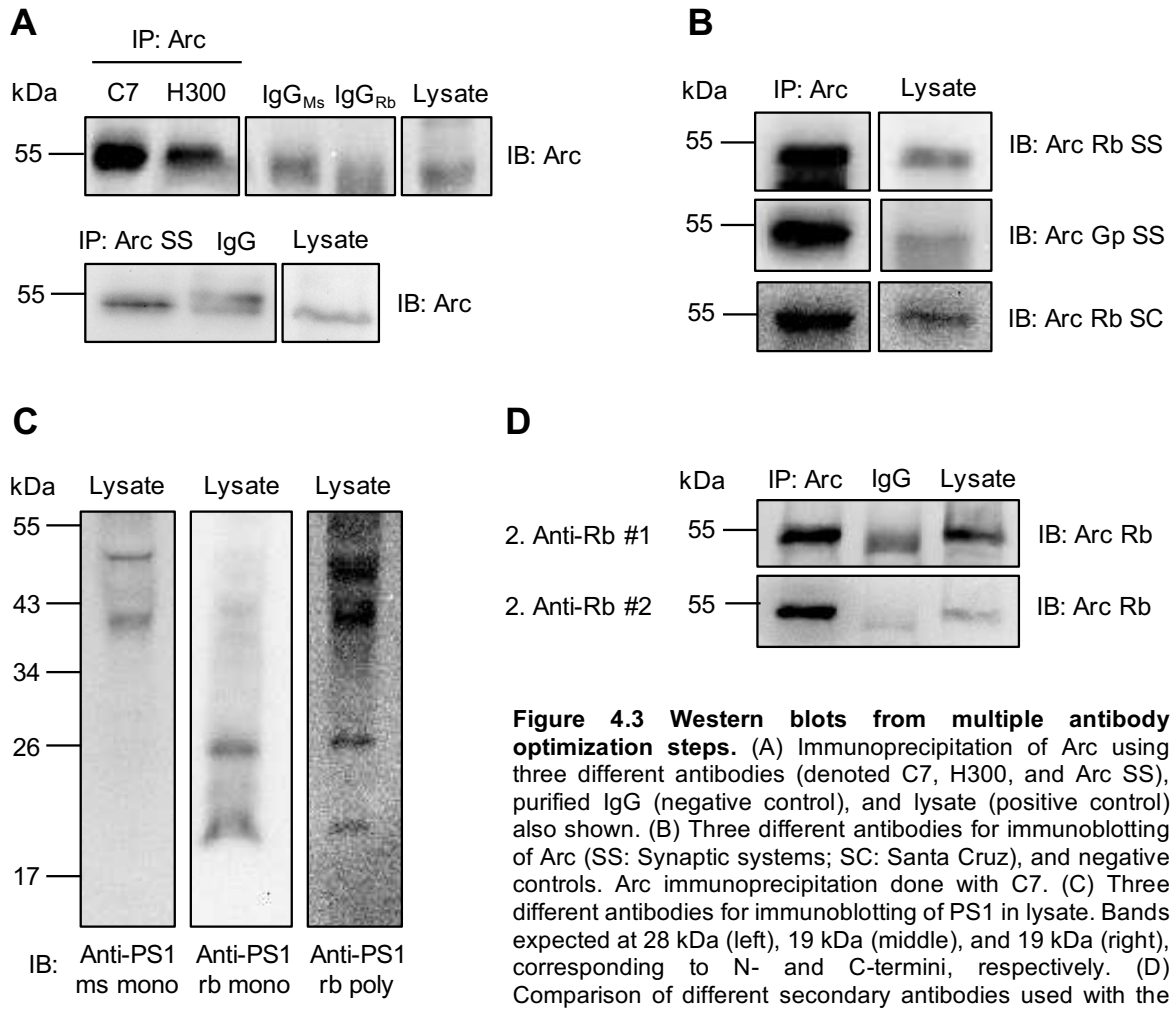

Figure 4.3 Western blots from multiple antibody optimization steps. (A) Immunoprecipitation of Arc using three different antibodies (denoted C7, H300, and Arc SS), purified IgG (negative control), and lysate (positive control) also shown. (B) Three different antibodies for immunoblotting of Arc (SS: Synaptic systems; SC: Santa Cruz), and negative controls. Arc immunoprecipitation done with C7. (C) Three different antibodies for immunoblotting of PS1 in lysate. Bands expected at 28 kDa (left), 19 kDa (middle), and 19 kDa (right), corresponding to N- and C-termini, respectively. (D) Comparison of different secondary antibodies used with the same primary antibody on the same membrane. #1 from Calbiochem, #2 from Santa Cruz biotech.

PS1. Bands at around 53 kDa were detected in both the rabbit polyclonal and the mouse monoclonal, corresponding to the size of the PS1 holoprotein. It also corresponds roughly to the size of the IgG heavy chain, and neither signal appeared as strong as the signal at 19 kDa, leading to the conclusion that the monoclonal rabbit anti-PS1 was the better choice of primary antibody, even though it recognizes the C-terminus, not the N-terminus which binds Arc, and might therefore have trouble recognizing whether PS1 was co-immunoprecipitated with Arc should the C-terminus dissociate from the N-terminus in the co-immunoprecipitation process. The N- and C-termini were, however, expected to stay in a complex with each other as well as with Arc until elution, and it was concluded that the monoclonal rabbit anti-PS1 should be used as the primary antibody in subsequent experiments.

Arc had acceptable candidates for primary antibody from rabbit and guinea pig; PS1 from rabbit. It was therefore decided to use the rabbit-derived antibody for Arc when both proteins were immunoprecipitated on the same gel, to allow use of the same secondary antibody.

Two different anti-rabbit secondary antibodies were tested in combination with immunoprecipitation with C7 and immunoblotting with rabbit anti-Arc selected in the earlier steps of the antibody selection process (Figure 4.3 D). Both secondary antibodies yielded bands in the Arc IP lanes (at 55 kDa, corresponding to Arc size) and in the IgG negative control (at 50 kDa, corresponding to the size of the heavy chain of IgG), but secondary antibody #1 (from Calbiochem) gave a much stronger signal in the IgG lane relative to the Arc IP lane, than did secondary antibody #2 (from Santa Cruz biotech); with the latter, a clear, strong band was seen in the Arc IP lane and only a relatively very weak one in the IgG lane.

4.2.2 Co-immunoprecipitation protocol test in WT mouse reveals need for optimization

With a set of antibodies selected, the protocol that had been used successfully on adult rat brain tissue was tested on mouse cortex to determine whether it was effective, and if so, efficient. Two sets of co-immunoprecipitation and reverse co-immunoprecipitation of Arc was attempted; one with Arc and calnexin (Cnx) as bait proteins, another with Arc and PSD-95 (PSD-95 being a known binding partner for Arc; calnexin being a suspected one). Membranes were then probed for either Arc and calnexin (Figure 4.4 A) or Arc and PSD-95 (Figure 4.4 B), to check for successful immunoprecipitation of the bait protein as well as co-immunoprecipitation of the other protein. Probing the first set of IPs for calnexin yielded a strong band in the calnexin IP at the same size as the input (~95 kDa), as well as a weak band

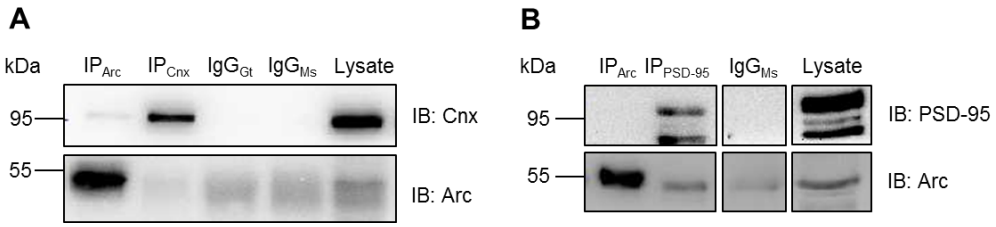

Figure 4.4 Testing co-immunoprecipitation protocol on WT mice. A co-immunoprecipitation protocol previously shown successful in adult rat brain (see appendix 1) was tested on WT mouse cortex. (A) Immunoprecipitation of Arc and calnexin, membrane probed for each one to check for immunoprecipitation and co-immunoprecipitation. (B) Immunoprecipitation of Arc and PSD-95, membrane probed for each one to check for immunoprecipitation and co-immunoprecipitation.

corresponding to the same size in the Arc IP, and no signal in the negative control, indicating successful co-immunoprecipitation of calnexin with Arc (Figure 4.4 A, top). Probing the second set of IPs for PSD-95 gave a band in the PSD-95 IP corresponding to the band in the input (~95 kDa), but none in the Arc IP, indicating no co-immunoprecipitation of Arc with PSD-95 (Figure 4.4 B, top). Probing for Arc revealed a strong band just below 55 kDa in both Arc IP lanes, consistent with Arc size, no clear band at the same height in the calnexin IP, and a clear, but slightly lower than 55 kDa band in the PSD-95 IP, corresponding to the size of the heavy chain of IgG. Membranes were also probed for PS1, dynamin 2 and syntaxin 4 to check for successful co-immunoprecipitation with Arc, but results were negative. The lack of co-immunoprecipitation of known or suspected binding partners with Arc indicated that optimization was needed before analyses of the APP/PS1 mice could be carried out reliably.

4.2.3 Adjusting the lysis buffer

The composition of the lysis buffer was varied in a set of experiments, with the objective to find a recipe that maximized the affinity of the target proteins toward each other and to minimize background signals in the visualization.

In one experiment, Arc immunoprecipitation was performed using four concentrations of sodium chloride (NaCl): 100 mM, 120 mM, 137 mM, and 150 mM (Figure 4.5 A) Visualization by Western blot revealed bands at expected Arc size (55 kDa), i.e. at equal height with the lysate positive control, in all four lanes. No substantial difference in intensity was detected between the four, thus all were considered equally effective. Varying the concentration of sodium fluoride (NaF) in addition to varying NaCl resulted in a weaker signal in the lane with IP performed using lysis buffer with 150 mM NaCl and 1 mM NaF than in the lane where 100 mM NaCl and 50 mM NaF was used; in addition, the latter conditions gave weaker signal in the IgG control lane (Figure 4.5 B). To further investigate the effect of varying

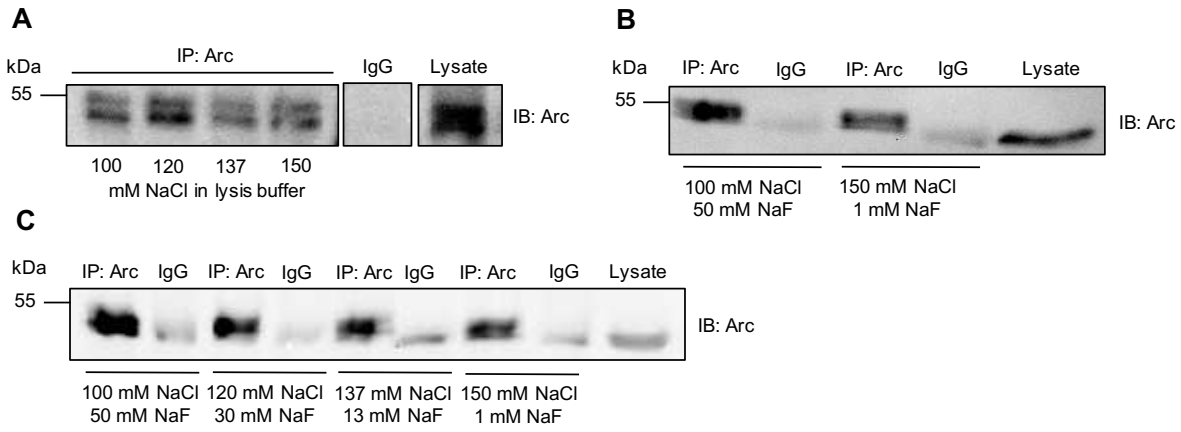

Figure 4.5 Varying lysis buffer salt concentrations. (A) Immunoprecipitation of Arc was carried out using lysis buffer with either 100 mM, 120 mM, 137 mM, or 150 mM NaCl. (B) NaCl and NaF concentrations were varied simultaneously, one IP being performed using lysis buffer with 100 mM NaCl and 50 mM NaF, and one using lysis buffer with 150 mM NaCl and 1 mM NaF. (C) IP of Arc carried out in lysis buffers with a range of variations in NaCl and NaF concentration.

NaCl and NaF concentration simultaneously, the experiment was repeated with additional variations: 120 mM NaCl and 30 mM NaCl, and 137 mM NaCl and 13 mM NaF. The strongest band was found in the lane with the Arc IP carried out using lysis buffer with 100 mM NaCl and 50 mM. Some signal at around the size of the IgG heavy chain was detected in the corresponding IgG control, but considerably weaker than in the Arc IP. Immunoblotting the Arc IP for PS1, dynamin 2, and syntaxin 4 still yielded negative results, therefore, the optimization process was continued with experiments varying several parameters in the co-immunoprecipitation procedure.

4.2.4 Optimizing the co-immunoprecipitation procedure

IgG controls were already included to control for non-specific protein binding to the IgG part of antibodies, but to investigate the extent of non-specific binding, a bead control was added to the mix; for this, protein G sepharose beads were only incubated with lysate, not antibody. Arc and calnexin co-IPs were performed with the bead control included (Figure 4.6). A band at 95 kDa in the Arc IP visible when blotting for calnexin suggested calnexin might have been

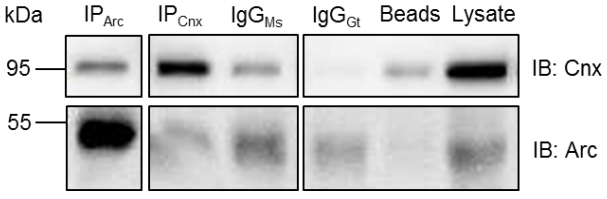

Figure 4.6 Checking for binding to beads. Arc and calnexin co-immunoprecipitations, immunoblotted for calnexin and Arc. Lane marked Beads contained elute from protein G sepharose beads not incubated with antibody, only lysate. Images in each row are from the same blot and exposure.

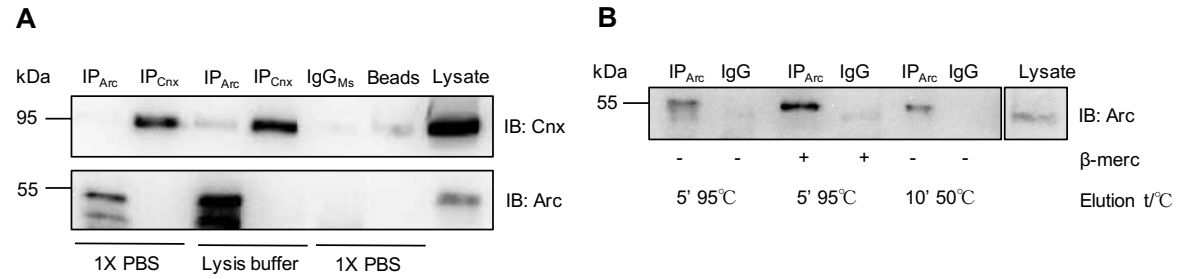

Figure 4.7 Varying blocking, washing, and elution protocols. (A) Co-immunoprecipitation of Arc and calnexin and vice versa was attempted in duplicate samples subjected to washing with two different reagents; little was in favor of co-immunoprecipitation success, but immunoprecipitation appeared effective. (B) Different elution protocols were tested on Arc IP, varying time and temperature of incubation with sample buffer and presence of β-mercaptoethanol in sample buffer.

co-immunoprecipitated with Arc, but almost equally strong bands in both IgG and bead control lanes indicated that it might only result from non-specific binding of calnexin to the beads and/or IgG chains, not association with Arc. Bead binding appeared to not be a problem in Arc IP. It was nevertheless decided that pre-incubation of beads with a blocking solution would be appropriate when performing immunoprecipitation of calnexin.

Beads were incubated with 5% BSA in 1X TBST for 30 min to avoid non-specific binding, and Arc and calnexin co-immunoprecipitations were again attempted (Figure 4.7 A). The co-immunoprecipitations were carried out in duplicates and subjected to different washing protocols, to study whether changing the stringency of the buffer used for washing the beads after incubation with lysate could increase the consistency and success rate of the co-immunoprecipitation protocol. Washing with lysis buffer yielded a considerably stronger immunoprecipitation signal than washing with 1X PBS. Interestingly, the band previously seen at 95 kDa in the Arc IP lane when blotting for calnexin was not seen in the Arc IP washed with 1X PBS, whereas it was present but not stronger than the bead control in the Arc IP washed with lysis buffer. IgG and bead controls were both washed with 1X PBS, and could consequently not be interpreted as accurate controls for the co-IPs washed with lysis buffer. However, given the increase in strength of signal in the lysis buffer-washed co-IPs relative to the 1X PBS-washed co-IPs, IgG and bead controls might also be expected to yield stronger bands at 95 kDa if washed with lysis buffer; potentially as strong as the one in the Arc IP lane.

Arc protein weighs in at 55 kDa, and as a consequence, any binding to the heavy chain of IgG, which could result from increased elution of antibodies from the beads with the proteins, has potential to obscure the results and confuse the interpreter. Different elution protocols were therefore tested for Arc IPs and accompanying IgG controls (Figure 4.7 B). Elution by incubation for 5 minutes at 95℃ in sample buffer with beta mercaptoethanol

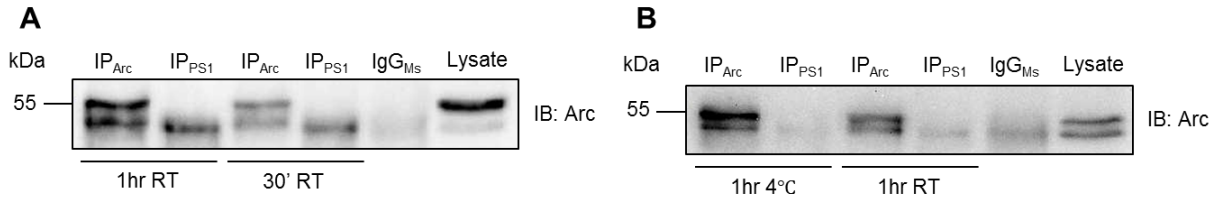

Figure 4.8 Varying IP incubation times and temperature. (A) Duplicates Arc and PS1 IPs carried out with variable incubation times were probed for Arc. In PS1 IP this gives a band at the expected size of the heavy chain of IgG. (B) Duplicates of Arc and PS1 IPs were carried out with further variation in incubation times, as well as temperature, and subsequently probed for Arc.

yielded a strong protein band at 55 kDa in the Arc IPs and little signal at 50 kDa in the IgG controls, and was the method used in subsequent experiments.

Incubating the sample with the antibody-bound beads for too long might lead to non-specific binding, but too little incubation time might decrease the yield to such a degree that neither non-specific nor specific interactions are strong enough to detect. Temperature also matters, as higher temperatures mean quicker movements at the molecular level and thus more chances of two proteins bumping into each other in a given time. The effect of these variables and the interplay between them was investigated with attempted co-immunoprecipitations of Arc and PS1, shown in Figure 4.8. The effectiveness of immunoprecipitation of Arc appeared to vary with time and temperature. When incubating the lysate with antibody-bound beads for either 30 minutes or 1 hour at room temperature (RT), the strongest signal at 55 kDa in the Arc IP blotted for Arc came from 1 hour incubation (A). A band of similar strength was found at 50 kDa in both Arc IPs and the paired PS1 IPs, as usual corresponding to the size of IgG's heavy chain; note, however, that the corresponding band in the IgG control lane was much weaker. The same co-immunoprecipitations were carried out with binding of the lysate to the antibody-beads for 1 hour at 4℃ or 1 hour at RT (B), yielding the strongest bands at 55 kDa when blotting for Arc in the Arc IP performed with 1 hour incubation in 4℃ Signal was present in all samples at 50 kDa, though at lower intensities and not in a pattern consistent with the ones in (A).

In addition to varying the length of incubation, one may also vary the sequence. All previous experiments were attempts at direct co-immunoprecipitation, where antibodies were first immobilized on the beads, then lysate was added. Indirect IP of Arc and PS1 were performed in duplicates with varying incubation times (Figure 4.9). They were expected to give more non-specific binding, but higher yield; the latter might compensate for the former in terms of utility of the information obtained. Antibodies incubated with lysate either

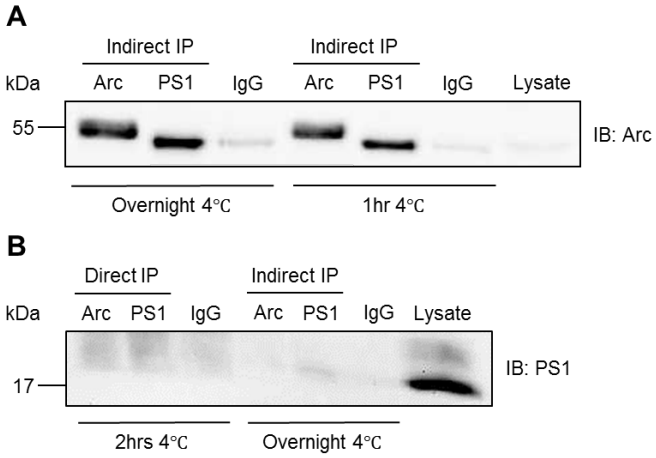

Figure 4.9 Indirect and direct co-immunoprecipitation. (A) Two sets of indirect co-immunoprecipitations with different duration of antibody and lysate incubation before addition of beads. When blotting for Arc, a strong band appears in the Arc IP and a similarly strong band slightly lower in the PS1 IP. (B) Two sets of co-immunoprecipitations carried out by either pre-binding antibody to beads then adding lysate or incubating all three reagents overnight. Immunoblotted for PS1.

overnight or one hour at 4℃ were washed once with 1X PBS and 2x with 1XPBST, then incubated with washed Protein G sepharose beads for 1 hour at 4℃ (A). A strong band was detected at ~50 kDa in the PS1 IP when blotting for Arc, similar to the bands at 50 kDa in other experiments earlier, but surprisingly strong; comparable in intensity to the band seen at 55 kDa in the Arc IP. IgG controls show only a weak band, as does the input. Immunoblotting was also performed with antibody against PS1 (monoclonal rabbit; epitope on the C-terminus), but no band was detected in the PS1 IP. Interestingly, though, in a comparison of direct (pre-binding of antibody to beads, then incubation with lysate for 2 hours at 4℃) and a variant of indirect immunoprecipitation (beads, antibody, and lysate incubated overnight at 4℃) and subsequent probing for PS1 with the monoclonal antibody against the C-terminus, the direct IP protocol yielded three similar bands in both Arc IP, PS1 IP, and IgG, whereas with the protocol where all reagents were added at the same time and incubated overnight, a single band corresponding to the size of the band seen in the lysate (the positive control) is recognizable in the lane loaded with the PS1 IP sample, but not, or if so only barely, in the Arc IP and IgG lanes. This supported the continued use of the protocol involving overnight incubation of beads, antibody, and lysate, and that it might be possible to achieve successful PS1 IP, if not Arc co-IP of PS1, in the samples from APP/PS1 mice, too. Immunoprecipitation of Arc appeared reliable with the present protocol, but given the similarity in size of Arc and the heavy chain of IgG, it was decided to switch to a secondary antibody in Western blotting that only recognized the light chain (25 kDa), thus hopefully minimizing the risk of confusion.

4.3 Co-immunoprecipitation of Arc and PS1 in WT and an AD model

Co-immunoprecipitation of Arc and PS1 was performed with frontal cortex tissue lysate from 7 months old male APP/PS1 mice and their WT littermates. All mice were housed in standard housing for 5 months, then one group had a running wheel introduced, another group a dummy wheel (non-functioning running wheel) introduced, while a third group remained in standard housing conditions. Mice were sacrificed and dissected at 7 months of age. Five sets of Arc and PS1 immunoprecipitations were carried out using the overnight immunoprecipitation protocol arrived at in the last section (as described in methods), proteins separated by SDS-PAGE and transferred to nitrocellulose membranes, and membranes then probed with antibodies against Arc and PS1 to check for (1) amount of immunoprecipitated protein and (2) possible co-immunoprecipitation of the other protein. Negative controls were included in the form of beads bound to IgG instead of a specific antibody and incubated with lysate, and beads incubated with only lysate (no antibody). Lysate from both strains of mice as positive controls, and an antibody control to which no lysate was added was included due to the suspicion that

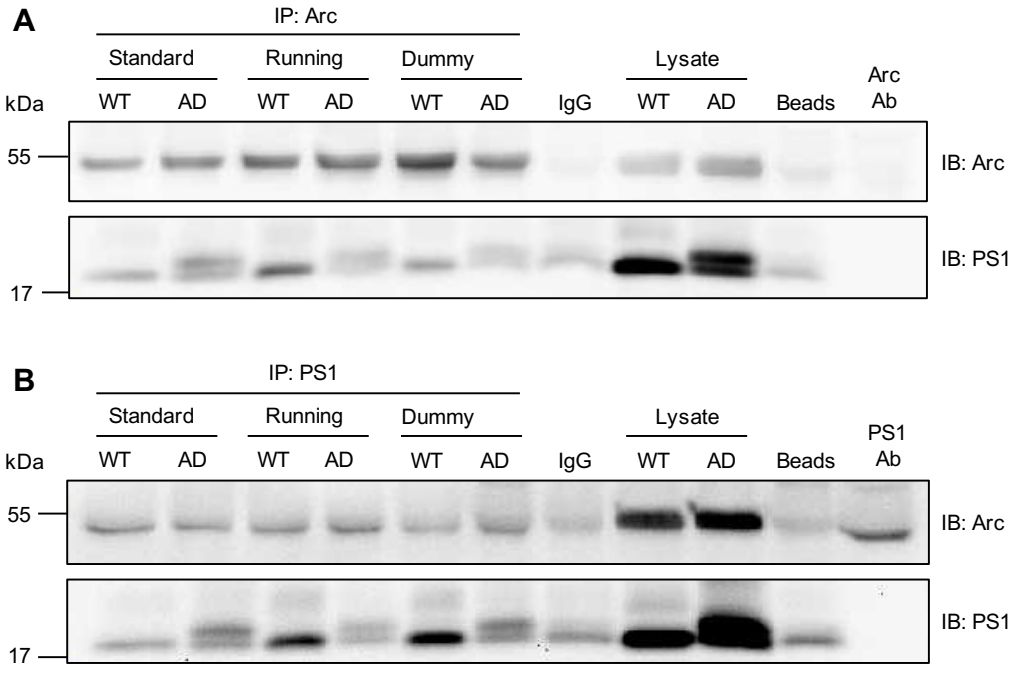

Figure 4.10 Western blots of Arc and PS1 co-immunoprecipitation in WT and APP/PS1 mice frontal cortex. (A) Immunoprecipitation of Arc and subsequent Western blotting for Arc (top) or PS1 (bottom). (B) Immunoprecipitation of PS1 and subsequent Western blotting for Arc (top) or PS1 (bottom). Material was lysed frontal cortex tissue from WT and APP/PS1 mice kept in standard housing, with a running wheel, or with a dummy wheel. Beads bound to IgG, beads not bound to antibody, and beads incubated with antibody but not lysate included as negative controls; lysate from both mouse strains included as positive control.

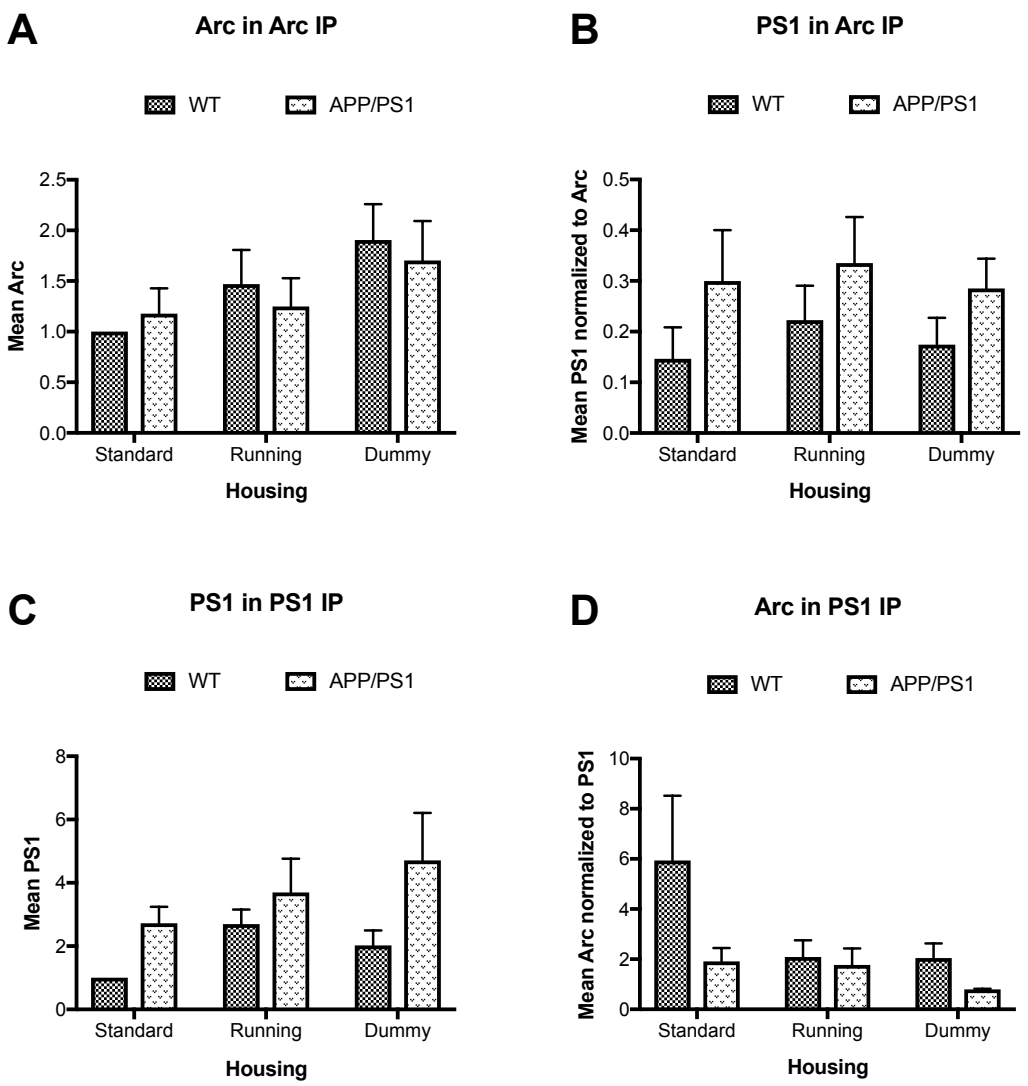

Figure 4.11 Means of Arc and PS1 immunoprecipitation and co-immunoprecipitation experiments in WT and APP/PS1 mouse frontal cortex. Plots comparing amount of protein detected with Western blotting in immunoprecipitations of Arc or PS1 in WT and APP/PS1 mice housed in three different conditions. (A) Mean amount of IP-ed Arc, all groups normalized to the amount of Arc IP-ed from the WT mouse in standard housing (n=5). (B) Mean amount of PS1 in Arc IPs, normalized to the amount of IP-ed Arc (n=5). (C) Mean amount of PS1 in PS1 IPs, normalized to the value for WT standard housing (n=5). (D) Mean amount of Arc in PS1 IPs, normalized to the amount of IP-ed PS1 (n=3). In quantification of PS1, both bands detected at ~18-19 kDa were included. Two-way ANOVA with multiple comparisons were performed, comparisons done (1) between different mouse strains housed together and (2) between groups of one mouse strain housed differently. All samples taken from frontal cortex. Error bars: SEM.

IgG heavy chains of the antibody used for PS1 immunoprecipitation was recognized as a band at 50 kDa in Western blots; see Figure 4.9. Representative blots are shown in Figure 4.10.

Lanes containing the Arc IPs consistently yielded bands at ~55 kDa when immunoblotted for Arc, and considerably weaker bands in IgG, bead, and antibody controls (Figure 4.10 A, top). Immunoblotting for PS1 in the Arc IPs yielded bands around the expected 18-19 kDa in all samples, but also in the IgG and bead controls, and these were of approximately the same intensity as the bulk of the bands detected in the Arc IP lanes (Figure

4.10 A, bottom). Interestingly, like in the expression analyses, probing with antibody against PS1 consistently yielded a double band in the lanes containing lysate from APP/PS1 mice, but only one (height of band corresponding to the lower of the double bands) in the WT mouse lanes. From simple visual inspection, there appeared to be no stable difference in intensity between the two bands originating from the transgenic mice.

Immunoblotting for Arc after immunoprecipitation of PS1 yielded bands of comparable intensity at around 50 kDa in all lanes, including in the IgG, the bead control, and the PS1 antibody control (though somewhat weaker in the IgG and bead control than in the rest) (Figure 4.10 B, top). As no lysate was incubated with the antibody control, the band cannot be a visualization of Arc; the bands in the other lanes must be interpreted in light of this. When probing for PS1 in the PS1 IPs, a similar pattern was seen to that of probing for PS1 in the Arc IPs; bands at the expected height for the PS1 C-terminus (18-19 kDa) were detected in all lanes, including the negative controls, except in the PS1 antibody control (Figure 4.10 B, bottom).. Again, the APP/PS1 mice consistently yielded double bands, the two bands in each lane being of roughly the same intensity.

Quantification and statistical analyses were performed on the four sets of images obtained after Western blot of the Arc and PS1 immunoprecipitations and attempted co-immunoprecipitations. Amount of Arc immunoprecipitated in each of five repetitions was estimated from quantification of Western blots. Values representing amount of immunoprecipitated Arc were normalized to the values for Arc in standard housing WT mice, and means plotted in Figure 4.11 (A). Amount of PS1 detected in five repetitions of Arc immunoprecipitations by probing with antibody against PS1 was quantified from Western blots. Values representing PS1 load were normalized to Arc load in the same lane, and mean values plotted in Figure 4.11 (B). The same experiments were carried out in reverse; PS1 immunoprecipitated and probed for PS1 and Arc, five repetitions (three for immunoblotting of Arc in PS1 IP) quantified and normalized to PS1 in WT standard housing or PS1 for the same lane, respectively. Plots of normalized mean values are shown in Figure 4.11 (C and D). Two-way ANOVA with multiple comparisons (Holm-Sidak) was performed separately on all four datasets, comparing (1) different mouse strains housed together and (2) differently housed groups of the same mouse strain. No statistically significant differences in amount of immunoprecipitated or potentially co-immunoprecipitated protein were found between the groups in either dataset.

4.4 GST pulldown

GST pulldown assay was introduced as a complimentary method to the co-immunoprecipitation, in an effort to increase the reliability of any obtained results by controlling for the possibility that they are an artifact of the method.

4.4.1 Protein purification

GST pulldown assays could not be performed without first producing purified GST and Arc conjugated to GST (GST-Arc). Bacteria were transformed with plasmids containing either the gene encoding GST or GST-Arc, grown, and the respective proteins were purified. Samples of GST or GST-Arc were collected at different stages in the purification process and separated on a polyacrylamide gel, then transferred to a membrane which was probed for GST (Figure 4.12). A strong band at the expected kDa for GST were detected in the samples from bacteria transformed with a plasmid containing the gene for GST, and a weak band at the expected kDa for GST-Arc in samples from bacteria transformed with a plasmid containing the gene for GST-Arc, suggesting successful purification, though with a higher yield of GST than GST-Arc.

Figure 4.12 GST/GST-Arc protein purification. Samples were collected at different stages of the GST-Arc and GST purification process: after lysis of the bacteria by sonication (left), after elution of the proteins from the filter column (middle), and after subsequent dialysis of the elute (right). Upon blotting with antibody against GST, GST-Arc and GST were expected to be detectable at the indicated heights.

4.4.2 Protocol established in rat brain tested for pulldown of PS1

As with the co-immunoprecipitation experiments, a GST pulldown assay demonstrated to be effective in rat brain tissue was established in the lab. The established protocol was selected as a basis for testing and potential optimization in mouse; first, however, it was tested in rat tissue in an attempt to replicate previous findings by other persons in the lab. GST pulldowns were performed with lysate form prefrontal cortex and naïve hippocampus from two adult rats (Figure 4.12). Ponceau staining of the membrane indicated similar loading of protein in GST and GST-Arc lanes (appendix 2). Immunoblotting for PS1 (N-terminal) revealed very weak bands close to the expected 28 kDa in the lanes where lysate was incubated with GST-Arc bound beads, but not in those where lysate was incubated with GST bound beads (negative

control). The protocol appeared successful in pulling down PS1 with GST-Arc, allowing for advancement to mouse tissue.

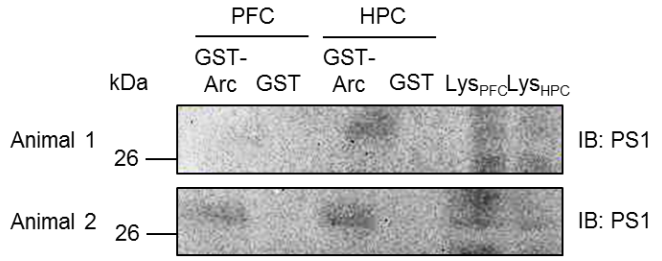

Figure 4.13 GST pulldown in rat prefrontal cortex and hippocampus. Weak bands were detected at the expected size for PS1 in the hippocampus of animal 1 and both the hippocampus and prefrontal cortex of animal 2. Contrast enhanced for visualization purposes (identical level of enhancement for both animals, originally on the same blot and thus the same image).

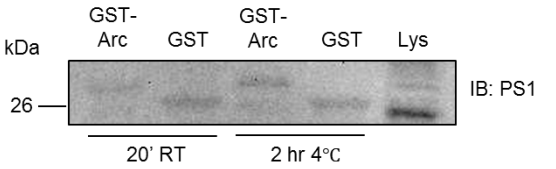

Figure 4.14 GST-Arc pulldown probed with PS1 Ms from abcam (expected band size: 28 kDa). Bands in GST-Arc sample lanes are at ~28 kDa, whereas bands in GST sample lanes are a little lower, at the expected size of GST (~26 kDa).

4.4.3 Applying the established protocol to mouse brain tissue

To control that the protocol was effective in mouse tissue as well as rat tissue and thus a feasible method for studying differences in PPIs in APP/PS1 and WT mice, it was applied to WT mouse hippocampus followed by Western blotting probing for PS1 (Figure 4.14). The duration and temperature of incubation of GST bound or GST-Arc bound beads with lysate was varied to investigate whether it changed the effectiveness of the protocol. All signals were weak, but a band at approximately 26 kDa was visible in lanes corresponding to the GST control, and much weaker but detectable in the GST-Arc pulldowns. A somewhat higher band was only present in the GST-Arc lanes, at similar strength in the two variants of the protocol. The positive control, i.e. the lane loaded with lysate, revealed only a weak, obscured band at the expected 28 kDa, but nevertheless a discernable one. Indications from the limited investigations were that the protocol was effective, if perhaps not efficient, in pulling down PS1 with GST-Arc, and might be applied successfully to studies of APP/PS1 mice in a future part of the overarching project.

5 Discussion

5.1 Interpreting the results

5.1.1 Arc expression did not differ significantly, but BDNF and PS1 did

To investigate potential differences in Arc, BDNF, and PS1 expression levels in APP/PS1 and WT mice kept in standard or enriched housing, frontal cortex tissue samples from each of the six groups of mice were separated with SDS-PAGE and immunoblotted for the proteins of interest. Five samples were obtained from each group of mice, allowing for statistical analysis of the quantified immunoblots. The results from the statistical analyses were largely in accordance with what has been described in the literature. Arc expression was not reported by the ANOVA analysis to be significantly influenced by either mouse strain or housing type; BDNF expression, however, was significantly increased in the mice given enriched environments the two last months of their life; PS1 expression, on the other hand, did not appear to be significantly influenced by a change of environment, but the mice genetically altered to express a PS1 mutant in addition to its endogenous PS1 did in fact display significantly higher expression of proteins recognized by the PS1 antibody than their wild type littermates.

The lack of changes in Arc expression was perhaps the least anticipated of the results three, as an increase in Arc has been reported in AD patients (Kerrigan and Randall, 2013). However, Arc expression is transient in nature because of the need for rapid, well timed, and specific regulation, thus a significant change in Arc dynamics in this particular AD model – should there be one – can be expected to be easier to capture if more precise and timed methods for stimulating activity were employed. The low n of the study might also well explain why no significant changes were detected; a higher "n" would effectively increase the sensitivity of the analysis and perhaps detect significant nuances that were not captured by this study.

It is no surprise that BDNF levels were significantly higher in the mice that had been kept in enriched environments for two months before sacrifice. It was, however, somewhat surprising that the increase did not appear to be larger with the introduction of a functional running wheel, than with a stationary one. One might expect that the introduction of both a novelty and physical activity would increase BDNF more than introduction of only one of those things, but that appeared to not be the case. Still, as with Arc, the statistical power of the study is very limited; the BDNF analyses were only based on 4 n, and further studies would

have to be carried out to be able to draw conclusions regarding the detailed implications of the results.

According to the statistics, PS1 expression was significantly higher in the transgenic mouse model than in the wild type mice. According to eyeballing, too, this seemed the case; the presence of a double band, both included when quantification the blots, in the APP/PS1 mice but not the WT, was a clear indication that there would be a detectable difference between the two groups statistically, too. The presence of this double band does, however, raise some concerns about validity. The proteins fragments from which the bands originated were not cut out of the gel and sequenced; it is therefore still unclear what they actually are. Still, given that the mouse strain contains genes for two variants of PS1, it is not unexpected that it could result in more than one variant of the C-terminus showing up in expression analyses, and other studies also report multiple bands representing C-terminal domain variants in Western blots of the same mutant (Cacquevel et al., 2012); it was therefore judged valid to include both bands in the quantification. Another question is what the use of such an analysis would be. It is not meaningless information, detecting alterations in PS1 expression in a mouse that has been genetically modified to have such alterations? Yes and no; the finding that it expresses more PS1 than its WT counterpart is perhaps *a priori* information and not very interesting, but alterations in expression with changing environment would have been. Additionally, the indication that it is in fact present in a higher amount has implications for the interpretation of data from protein-protein interaction studies involving PS1, making it relevant information indeed for later parts of this study.

5.1.2 Further tweaking required for robust co-immunoprecipitation

The optimization process for the co-immunoprecipitation protocol has a number of different steps, and part of the ambition of the process was to introduce variables in a sequence that would decrease the risk that changing one variable would render conclusions from the previous steps invalid. This had to be an ambition, because it was not feasible to test all possible combinations of all the different variables.

The antibody optimization was the first step, as a functioning antibody was a requirement for the whole of the rest of the process. Anti-Arc C7 was shown to be effective, and kept as the main antibody for immunoprecipitating Arc throughout the process. Anti-Arc H300 was also shown to be effective, but as the manufacturer has stopped the production, C7 was the preferred choice. For the Western blotting, both effective primary and secondary antibodies were needed, and the combinations of these with each other and with the

immunoprecipitation antibody had to both make sense theoretically and work practically. As for the primary antibodies against Arc, the results indicated that there were more than one efficient alternative, resulting in the pleasing situation of having options, practical should a subsequent step in the optimization process render one of the options unsuitable. This may be the case for rabbit anti-Arc (Synaptic systems). Using it as a primary antibody to blot for Arc in a reverse co-immunoprecipitation of arc carried out with mouse anti-PS1 (Abcam) has been demonstrated to result in a band at almost the same height as Arc would be expected to be found, even if it is not exposed to lysate (see Figures 4.9 and 4.10). In an experiment not documented here, immunoblotting with anti-Arc C7 did not do the same in combination with rabbit anti-PS1 (Abcam) used for IP. However, because the mouse anti-PS1 was the only PS1 antibody specifically targeting the N-terminal domain (i.e. the part that binds Arc) the lab was able to track down commercially at the time the experiments were carried out, it was decided that it was the best option for maximizing chances of successful Arc co-immunoprecipitation. It has not proven particularly successful as of yet, and given the fact that the two domains of PS1 stay associated (Wolfe, 2006), future studies may have something to gain from reversing that decision. The propensity of the two domains of PS1 to stay associated after endoproteolysis means that they should both be possible to co-immunoprecipitate with Arc; perhaps an antibody targeting the C-terminus is indeed a better choice than that made in this project. Secondary antibodies were also a factor in the attempt to avoid unwanted background signals, particularly those corresponding the size of the IgG heavy chain and to a minor degree the light chain (because of the unfortunate similarity in size of Arc (55 kDa) with the heavy chain (50 kDa)). Measures were taken to avoid both background signals and non-specific binding of proteins to the beads (as opposed to specifically to the antibodies); e.g. changing the secondary antibody, blocking the beads with BSA; and these were demonstrated to be relatively successful.

The preliminary tests of the co-immunoprecipitation protocol in mice were, however, not successful, leading to a process of tweaking lysis buffer composition and changing duration and temperature of the incubation steps, etc. An optimized lysis buffer is important for the success of the co-immunoprecipitation, as protein-protein interactions may be transient and hard to capture, and while performing the experiments under physiological conditions seems a logical starting point, conditions are variable even in cells (e.g. changes in pH, calcium concentration in a neuron as a consequence of signaling, etc.). Altering conditions a little to facilitate more interaction is therefore not inherently “wrong” in the sense of not valid, one

just has to be conscious of what it entails; e.g. in what calcium concentrations will these proteins interact; and how to interpret any results.

Negative controls were added to control for non-specific binding, one of them being the bead control where no antibody was added, only lysate. It is debatable whether this is a valid control; the IgG with no epitope bound to the beads should be expected to be a more relevant control, mimicking the conditions of the immunoprecipitation samples, only specifically without the antigen binding properties.

The optimization steps led to a protocol, the effectiveness of which was still debatable. Immunoprecipitation of Arc was, however, stable and consistent, and the project moved on to the studies of AD model mice.

5.1.3 Co-immunoprecipitation of Arc and PS1 appeared unsuccessful in APP/PS1 and WT mice

Bidirectional co-immunoprecipitations of Arc and PS1 were carried out in repeats of five, using the protocol arrived at through the optimization process. This yielded four categories of immunoblots: Arc immunoprecipitations blotted for Arc, Arc immunoprecipitations blotted for PS1, PS1 immunoprecipitations blotted for PS1, and PS1 immunoprecipitations blotted for Arc. Two aspects of the results were analyzed; first, whether the co-immunoprecipitations were successful or not, and second, whether there were statistically significant variations between the amount of protein detected in different groups of mice.

Arc IP blotted for Arc looked successful, the signal in the IP lanes much stronger than any of the negative controls. Signal in the negative controls may be explained as Arc binding non-specifically to beads or the heavy or light chain of the antibodies, but specific binding to the Arc antibody appeared consistently stronger and were therefore interpreted as successful IP. If PS1 was successfully co-immunoprecipitated with Arc, probing for PS1 in the Arc IP would yield bands corresponding to PS1 size in the IP lanes, but not in the control lanes. This was not found to be the case. While the now-characteristic double band at 18-19 kDa was clearly discernable in the blots, bands of similar intensity were present in the controls, too, indicating that PS1 did associate with something in the bead-antibody complex during the co-immunoprecipitation process, but not necessarily with Arc. It might associate with Arc, too, but a specific interaction was not detected in these experiments.

Immunoprecipitation of PS1 and subsequent blotting with anti-PS1 produced similar results to those obtained when probing for PS1 in the Arc IP, indicating that PS1 was not successfully immunoprecipitated, and that bands detected in the ECL visualization were a

result of PS1 binding non-specifically to either beads and/or the IgG part of the antibodies. Given that the PS1 IP was not judged successful, Arc was not expected to have been co-immunoprecipitated in this set of experiments. Nevertheless, membranes were probed with anti-Arc, only to confirm that the band visible at around 50-55 kDa could not be interpreted as Arc, as the band was present at equal strength in the antibody control. With evidence accumulating in favor of this, it was clear that a different antibody or combination of antibodies was needed to successfully investigate this proposed interaction before being able to draw conclusions of how Arc may have altered activity in the regulation of the γ-secretase complex in APP/PS1 mice.

5.1.4 Neither housing nor mouse strain explained variation in Arc and PS1 immunoprecipitated from WT and APP/PS1 mice

The signals corresponding to expected weight for Arc or PS1 in each one of the just described Arc or PS1 blots were measured and used for statistical analyses. Multiple comparisons performed on the data did not reveal any significant relationships between the mice with the same genetic makeup but with different housing, nor between the mice with different genetic makeup but the same housing conditions. As concluded above, only the Arc immunoprecipitation was believed to have achieved what it set out to do, therefore any statistically significant results from the other sets of blots would have not been theoretically meaningful. However, it is important to stress that the handling of the data pre-statistics could have a considerable influence on the conclusions drawn from them. Here, the values measured after blotting for PS1 in Arc IP, or vice versa, were normalized to the corresponding value for the immunoprecipitated protein. Originally, they were also normalized to the value for the wild type mouse kept in standard housing throughout its life. This yielded some surprisingly, and suspiciously, significant results because the SEM was very high for the mean value of Arc in PS1 IP, and as that was effectively defined as one, the SEM was lost. Like in the expression analyses (5.1.1), the n was relatively low here (n=3 for Arc in PS1 IP, n=5 for the rest. Although no statistically significant patterns were found, the plots (Figure 4.11) , particularly A and C, were suggestive of a general pattern where housing enrichment entailed an increasing amounts of protein being immunoprecipitated . This might be investigated further by repeating the experiments more times.

5.1.5 GST-Arc might successfully pull down PS1

Perhaps the most successful part of the project was the smallest one; preliminary GST-Arc pulldown experiments in both rat and mouse suggested, though the signals were very weak, that PS1 preferentially associated with the sepharose bead-immobilized GST-Arc than with a GST control. Note, however, that more repetitions are needed to determine whether the positive results were coincidences.

5.2 Answering the hypotheses

At the end of the theoretical introduction to this project I deduced a set of concrete hypotheses that might be supported or not supported after analysis of the data obtained during the project.

H1 Arc protein expression in the brain before external stimulus < Arc protein expression in the brain after external stimulus

Analysis of the expression data indicated no statistically significant relationship between Arc protein expression and the two operationalizations of external stimulus; presence of a running wheel and presence of a dummy wheel; in other words, H1 is not supported.

H2 Stimulus-induced change in Arc protein expression in healthy individuals > stimulus-induced change in Arc expression in individuals with AD

The form of stimulus (running wheel and dummy wheel (a novelty introduction)) presented to the mice in these experiments did not appear to have a significant effect on Arc protein expression, as measured in frontal cortex tissue lysate, in either mouse strain. Amount of Arc immunoprecipitated from the same tissue sample was also not significantly altered with the stimulus. H2 is thus not supported by the experimental data from this project.

H3 Arc/PS1 interaction in healthy brains < Arc/PS1 interaction in AD brains

No reliable data was obtained about an interaction between Arc and PS1 in this project, therefore, H3 is not supported.

5.3 Reliability and validity

In the methodological discussion in the introduction, it was decided that an animal model was the appropriate choice for answering the hypotheses of this thesis, heavily influenced also by restrictions stemming from the ambition to integrate the thesis project with a larger collaboration. Arguments in favor of using an animal model is that they are generally useful in AD research because AD is a slow progressing disease, hence it is not always feasible to use patient material. Patient-derived material also entails the possibility of co-morbidities affecting the results; using a model system decreases the number of variables. However, using a model system should always raise the question of validity. The particular model used in the present project is a model of Aβ pathology, based on known FAD mutations directly involved in amyloidosis; other features of AD, such as tau pathology (limited in the model), are not necessarily represented as they appear in patients. Investigating PS1 in a model where it is one of the introduced mutations can also be argued to decrease the generalizability of the information obtained.

In addition to validity, the reliability of model system may be a concern. Female mice might produce different results depending on their menstrual cycle; male mice were used in the experiments on APP/PS1 to avoid such issues, but other things may influence the reliability of the model and subsequent comparability of results, like variations in the local microbiota. Different labs and animal facilities have different microbiomes, potentially accounting for part of the conflicting results in biomedical research. However, that is also the case for the rest of the world, so any robust effects would hopefully still be replicable.

One could also argue that any *in vivo* model system is too complex, and that it would have been more appropriate to do preliminary studies of the interaction between Arc and PS1 *in vitro*, even though later work on e.g. LTP and behavior favor an animal model. It would also be possible to increase specificity and decrease variables within the available framework. To account for the local variability in Arc expression associated with Aβ pathology, synaptoneurosomes might have been a good choice. The methods used here do not have high enough resolution to account for the local differences presented by Rudinskiy et al. (2012).

The methods also have technical limitations which can influence both reliability and validity. This study relied heavily on antibodies, and their ineffectiveness and/or inappropriateness was the cause of many a struggle, as described in earlier paragraphs. Others who have reported successful immunoprecipitation of PS1 have used non-commercial antibodies, making replication near impossible.

GST pulldown was to be used as a supplementing method, controlling for potential artefacts grounded in the method. However, both the co-immunoprecipitation and the GST pulldown procedures relied on Western blotting for visualization, meaning that the strategy did not allow me to control for artifacts of the WB step.

Processing the data, i.e. quantification and statistical analysis, introduced another set of uncertainties. Quantification was done manually, demanding that the judgments of e.g. what is background noise and what is not, what is the protein of interest and what is not, were correct. It is safe to assume this was not always the case. As noted previously, the low n of the project is also an issue.

5.4 Conclusions and thoughts on further research

The aims of the project was partially completed. The intended expression analyses and immunoprecipitations were carried out, but the development of an optimized co-immunoprecipitation protocol for the study of Arc/PS1 interaction in mice was not successful. Results of the analyses of expression of three proteins in the brain of a model system for Alzheimer's disease demonstrated that BDNF levels increase in response to enrichment of the environment and physical activity, but did not support a significant role for Arc studied in this particular framework, nor did results from immunoprecipitation of Arc from the same mouse brains. However, extensive literature describes a role of Arc in AD, mainly as a propagator of the disease through promotion of LTD and involvement in regulating Aβ generation(Wu et al., 2011). The absence of results indicating Arc dysfunction in AD in this project may reflect reality, but may also be a consequence by limitations in the sensitivity and specificity of the methodological approach, and further investigations are therefore necessary before drawing conclusions of either kind. The resolution of the experimental set-up could be enhanced, e.g. by studying synaptoneurosomes instead of whole brain regions. Carrying out the same experiments in different brain regions important for different types of memory could also unveil nuances not captured here, like the hippocampus and amygdala. An important aspect of Arc relation to AD is the regulation of pathways leading to Aβ generation, and to understand the relationship between Arc and AD pathology, future research should include investigations into Aβ load, ideally to the resolution of soluble oligomers.

As the field of Alzheimer's research is, like its subjects of study, growing older, it luckily does not show signs of cognitive decline; on the contrary. The neuronal network of AD research is growing and spreading, making connections to other fields. Tough nuts to

crack, Alzheimer's disease and other neurodegenerative disorders are still a long way from being cured, but continued curiosity and relentless work will bring us ever closer.

References

Alzheimer, A. (1987). About a peculiar disease of the cerebral cortex. By Alois Alzheimer, 1907 (Translated by L. Jarvik and H. Greenson). Alzheimer disease and associated disorders *1*, 3-8.

Azevedo, F.A., Carvalho, L.R., Grinberg, L.T., Farfel, J.M., Ferretti, R.E., Leite, R.E., Jacob Filho, W., Lent, R., and Herculano-Houzel, S. (2009). Equal numbers of neuronal and nonneuronal cells make the human brain an isometrically scaled-up primate brain. The Journal of comparative neurology *513*, 532-541.

Bahrami, S., and Drabløs, F. (2016). Gene regulation in the immediate-early response process. Advances in Biological Regulation *62*, 37-49.

Bai, X.-c., Yan, C., Yang, G., Lu, P., Ma, D., Sun, L., Zhou, R., Scheres, S.H.W., and Shi, Y. (2015). An atomic structure of human [ggr]-secretase. Nature *525*, 212-217.

Bali, J., Halima, S.B., Felmy, B., Goodger, Z., Zurbriggen, S., and Rajendran, L. (2010). Cellular basis of Alzheimer's disease. Annals of Indian Academy of Neurology *13*, S89-S93.

Bartsch, T., and Wulff, P. (2015). The hippocampus in aging and disease: From plasticity to vulnerability. Neuroscience *309*, 1-16.

Bekinschtein, P., Cammarota, M., Katche, C., Slipczuk, L., Rossato, J.I., Goldin, A., Izquierdo, I., and Medina, J.H. (2008). BDNF is essential to promote persistence of long-term memory storage. Proceedings of the National Academy of Sciences *105*, 2711-2716.

Bi, R., Kong, L.-L., Xu, M., Li, G.-D., Zhang, D.-F., Li, T., Fang, Y., Zhang, C., Zhang, B., and Yao, Y.-G. (2017). The Arc Gene Confers Genetic Susceptibility to Alzheimer's Disease in Han Chinese. Molecular Neurobiology, 1-10.

Bramham, C.R. (2007). Control of synaptic consolidation in the dentate gyrus: mechanisms, functions, and therapeutic implications. Progress in brain research *163*, 453-471.

Bramham, C.R., Alme, M.N., Bittins, M., Kuipers, S.D., Nair, R.R., Pai, B., Panja, D., Schubert, M., Soule, J., Tiron, A.*, et al.* (2010). The Arc of synaptic memory. Experimental Brain Research Experimentelle Hirnforschung Experimentation Cerebrale *200*, 125-140.

Bramham, C.R., and Messaoudi, E. (2005). BDNF function in adult synaptic plasticity: The synaptic consolidation hypothesis. Progress in Neurobiology *76*, 99-125.

Bramham, C.R., and Wells, D.G. (2007). Dendritic mRNA: transport, translation and function. Nat Rev Neurosci *8*, 776-789.

Bramham, C.R., Worley, P.F., Moore, M.J., and Guzowski, J.F. (2008). The immediate early gene arc/arg3.1: regulation, mechanisms, and function. The Journal of neuroscience : the official journal of the Society for Neuroscience *28*, 11760-11767.

Braak, H., and Braak, E. (1991). Neuropathological stageing of Alzheimer-related changes. Acta neuropathologica *82*, 239-259.

Braak, H., and Braak, E. (1997). Frequency of Stages of Alzheimer-Related Lesions in Different Age Categories. Neurobiology of Aging *18*, 351-357.

Buzsáki, G. (1996). The Hippocampo-Neocortical Dialogue. Cerebral Cortex *6*, 81-92.

Cacquevel, M., Aeschbach, L., Houacine, J., and Fraering, P.C. (2012). Alzheimer's Disease-Linked Mutations in Presenilin-1 Result in a Drastic Loss of Activity in Purified γ-Secretase Complexes. PLOS ONE *7*, e35133.

Chowdhury, S., Shepherd, J.D., Okuno, H., Lyford, G., Petralia, R.S., Plath, N., Kuhl, D., Huganir, R.L., and Worley, P.F. (2006). Arc/Arg3.1 Interacts with the Endocytic Machinery to Regulate AMPA Receptor Trafficking. Neuron *52*, 445-459.

Christensen, D.Z., Thomsen, M.S., and Mikkelsen, J.D. (2013). Reduced basal and novelty-induced levels of activity-regulated cytoskeleton associated protein (Arc) and c-Fos mRNA in the cerebral cortex and hippocampus of APPswe/PS1ΔE9 transgenic mice. Neurochemistry International *63*, 54-60.

Craig, L.A., Hong, N.S., and McDonald, R.J. (2011). Revisiting the cholinergic hypothesis in the development of Alzheimer's disease. Neuroscience & Biobehavioral Reviews *35*, 1397-1409.

Cummings, J., Aisen, P.S., DuBois, B., Frölich, L., Jack, C.R., Jones, R.W., Morris, J.C., Raskin, J., Dowsett, S.A., and Scheltens, P. (2016). Drug development in Alzheimer's disease: the path to 2025. Alzheimer's Research & Therapy *8*, 39.

Davies, C.A., Mann, D.M.A., Sumpter, P.Q., and Yates, P.O. (1987). A quantitative morphometric analysis of the neuronal and synaptic content of the frontal and temporal cortex in patients with Alzheimer's disease. Journal of the Neurological Sciences *78*, 151-164.

De Strooper, B., and Karran, E. (2016). The Cellular Phase of Alzheimer's Disease. Cell *164*, 603-615.

De-Paula, V.J., Radanovic, M., Diniz, B.S., and Forlenza, O.V. (2012). Alzheimer's disease. Sub-cellular biochemistry *65*, 329-352.

Di Marco, L.Y., Venneri, A., Farkas, E., Evans, P.C., Marzo, A., and Frangi, A.F. (2015). Vascular dysfunction in the pathogenesis of Alzheimer's disease--A review of endothelium-mediated mechanisms and ensuing vicious circles. Neurobiology of disease *82*, 593-606.

Dorszewska, J., Prendecki, M., Oczkowska, A., Dezor, M., and Kozubski, W. (2016). Molecular Basis of Familial and Sporadic Alzheimer's Disease. Current Alzheimer research *13*, 952-963.

Duyckaerts, C. (2011). Tau pathology in children and young adults: can you still be unconditionally baptist? Acta neuropathologica *121*, 145-147.

Eichenbaum, H. (2004). Hippocampus: cognitive processes and neural representations that underlie declarative memory. Neuron *44*, 109-120.

Evin, G., and Hince, C. (2013). BACE1 as a therapeutic target in Alzheimer's disease: rationale and current status. Drugs & aging *30*, 755-764.

Fraering, P.C., Ye, W., Strub, J.-M., Dolios, G., LaVoie, M.J., Ostaszewski, B.L., van Dorsselaer, A., Wang, R., Selkoe, D.J., and Wolfe, M.S. (2004). Purification and Characterization of the Human γ-Secretase Complex. Biochemistry *43*, 9774-9789.

Fromer, M., Pocklington, A.J., Kavanagh, D.H., Williams, H.J., Dwyer, S., Gormley, P., Georgieva, L., Rees, E., Palta, P., Ruderfer, D.M.*, et al.* (2014). De novo mutations in schizophrenia implicate synaptic networks. Nature *506*, 179-184.

Gengler, S., Hamilton, A., and Holscher, C. (2010). Synaptic plasticity in the hippocampus of a APP/PS1 mouse model of Alzheimer's disease is impaired in old but not young mice. PLoS One *5*, e9764.

Giannakopoulos, P., Herrmann, F.R., Bussiere, T., Bouras, C., Kovari, E., Perl, D.P., Morrison, J.H., Gold, G., and Hof, P.R. (2003). Tangle and neuron numbers, but not amyloid load, predict cognitive status in Alzheimer's disease. Neurology *60*, 1495-1500.

Gu, L., and Guo, Z. (2013). Alzheimer's Abeta42 and Abeta40 peptides form interlaced amyloid fibrils. J Neurochem *126*, 305-311.

Guntupalli, S., Widagdo, J., and Anggono, V. (2016). Amyloid-β-Induced Dysregulation of AMPA Receptor Trafficking. Neural Plasticity *2016*, 12.
Hardy, J.A., and Higgins, G.A. (1992). Alzheimer's disease: the amyloid cascade hypothesis. Science *256*, 184-185.
Hebb, D.O. (1949). The organization of behavior: A neuropsychological theory. (New York: John Wiley and Sons, Inc.).
Hoe, H.-S., Lee, H.-K., and Pak, D.T.S. (2012). The Upside of APP at Synapses. CNS neuroscience & therapeutics *18*, 47-56.
Hsieh, H., Boehm, J., Sato, C., Iwatsubo, T., Tomita, T., Sisodia, S., and Malinow, R. (2006). AMPA-R Removal Underlies Aβ-induced Synaptic Depression and Dendritic Spine Loss. Neuron *52*, 831-843.
Huentelman, M.J., Muppana, L., Corneveaux, J.J., Dinu, V., Pruzin, J.J., Reiman, R., Borish, C.N., De Both, M., Ahmed, A., Todorov, A.*, et al.* (2015). Association of SNPs in EGR3 and ARC with Schizophrenia Supports a Biological Pathway for Schizophrenia Risk. PLoS One *10*, e0135076.
Haass, C., Kaether, C., Thinakaran, G., and Sisodia, S. (2012). Trafficking and proteolytic processing of APP. Cold Spring Harb Perspect Med *2*, a006270.
Haass, C., and Selkoe, D.J. (2007). Soluble protein oligomers in neurodegeneration: lessons from the Alzheimer's amyloid [beta]-peptide. Nat Rev Mol Cell Biol *8*, 101-112.
Iljina, M., Garcia, G.A., Dear, A.J., Flint, J., Narayan, P., Michaels, T.C.T., Dobson, C.M., Frenkel, D., Knowles, T.P.J., and Klenerman, D. (2016). Quantitative analysis of co-oligomer formation by amyloid-beta peptide isoforms. Scientific Reports *6*, 28658.
Kamenetz, F., Tomita, T., Hsieh, H., Seabrook, G., Borchelt, D., Iwatsubo, T., Sisodia, S., and Malinow, R. (2003). APP processing and synaptic function. Neuron *37*, 925-937.
Kerrigan, T.L., and Randall, A.D. (2013). A new player in the 'synaptopathy' of Alzheimer's disease - Arc/Arg 3.1. Frontiers in neurology *4*.
Kim, J., Basak, J.M., and Holtzman, D.M. (2009). The Role of Apolipoprotein E in Alzheimer's Disease. Neuron *63*, 287-303.
Kimberly, W.T., LaVoie, M.J., Ostaszewski, B.L., Ye, W., Wolfe, M.S., and Selkoe, D.J. (2003). γ-Secretase is a membrane protein complex comprised of presenilin, nicastrin, aph-1, and pen-2. Proceedings of the National Academy of Sciences *100*, 6382-6387.
Klevanski, M., Herrmann, U., Weyer, S.W., Fol, R., Cartier, N., Wolfer, D.P., Caldwell, J.H., Korte, M., and Muller, U.C. (2015). The APP Intracellular Domain Is Required for Normal Synaptic Morphology, Synaptic Plasticity, and Hippocampus-Dependent Behavior. The Journal of neuroscience : the official journal of the Society for Neuroscience *35*, 16018-16033.
Konietzko, U. (2012). AICD nuclear signaling and its possible contribution to Alzheimer's disease. Current Alzheimer research *9*, 200-216.
Korb, E., Wilkinson, C.L., Delgado, R.N., Lovero, K.L., and Finkbeiner, S. (2013). Arc in the nucleus regulates PML-dependent GluA1 transcription and homeostatic plasticity. Nature neuroscience *16*.
Kuipers, S.D., and Bramham, C.R. (2006). Brain-derived neurotrophic factor mechanisms and function in adult synaptic plasticity: new insights and implications for therapy. Current opinion in drug discovery & development *9*, 580-586.
Kumar, D.K.V., Choi, S.H., Washicosky, K.J., Eimer, W.A., Tucker, S., Ghofrani, J., Lefkowitz, A., McColl, G., Goldstein, L.E., Tanzi, R.E.*, et al.* (2016). Amyloid-β peptide protects against microbial infection in mouse and worm models of Alzheimer's disease. Science Translational Medicine *8*, 340ra372.
Lacor, P.N., Buniel, M.C., Chang, L., Fernandez, S.J., Gong, Y., Viola, K.L., Lambert, M.P., Velasco, P.T., Bigio, E.H., Finch, C.E.*, et al.* (2004). Synaptic Targeting by

Alzheimer's-Related Amyloid β Oligomers. The Journal of Neuroscience *24*, 10191.

Landgren, S., von Otter, M., Palmer, M.S., Zetterstrom, C., Nilsson, S., Skoog, I., Gustafson, D.R., Minthon, L., Wallin, A., Andreasen, N.*, et al.* (2012). A novel ARC gene polymorphism is associated with reduced risk of Alzheimer's disease. Journal of neural transmission (Vienna, Austria : 1996) *119*, 833-842.

Lee, H.-g., Perry, G., Moreira, P.I., Garrett, M.R., Liu, Q., Zhu, X., Takeda, A., Nunomura, A., and Smith, M.A. (2005). Tau phosphorylation in Alzheimer's disease: pathogen or protector? Trends in Molecular Medicine *11*, 164-169.

Lin, T.W., Shih, Y.H., Chen, S.J., Lien, C.H., Chang, C.Y., Huang, T.Y., Chen, S.H., Jen, C.J., and Kuo, Y.M. (2015). Running exercise delays neurodegeneration in amygdala and hippocampus of Alzheimer's disease (APP/PS1) transgenic mice. Neurobiology of learning and memory *118*, 189-197.

Majbour, N.K., Chiasserini, D., Vaikath, N.N., Eusebi, P., Tokuda, T., van de Berg, W., Parnetti, L., Calabresi, P., and El-Agnaf, O.M.A. (2017). Increased levels of CSF total but not oligomeric or phosphorylated forms of alpha-synuclein in patients diagnosed with probable Alzheimer's disease. Scientific Reports *7*, 40263-40263.

Masters, C.L., Bateman, R., Blennow, K., Rowe, C.C., Sperling, R.A., and Cummings, J.L. (2015). Alzheimer's disease. Nature Reviews Disease Primers *1*, 15056.

Messaoudi, E., Kanhema, T., Soulé, J., Tiron, A., Dagyte, G., da Silva, B., and Bramham, C.R. (2007). Sustained Arc/Arg3.1 Synthesis Controls Long-Term Potentiation Consolidation through Regulation of Local Actin Polymerization in the Dentate Gyrus <em>In Vivo</em&gt. The Journal of Neuroscience *27*, 10445.

Morales, R., Bravo-Alegria, J., Duran-Aniotz, C., and Soto, C. (2015). Titration of biologically active amyloid–β seeds in a transgenic mouse model of Alzheimer's disease. Scientific Reports *5*, 9349.

Mullan, M., Crawford, F., Axelman, K., Houlden, H., Lilius, L., Winblad, B., and Lannfelt, L. (1992). A pathogenic mutation for probable Alzheimer's disease in the APP gene at the N-terminus of beta-amyloid. Nature genetics *1*, 345-347.

Myrum, C., Baumann, A., Bustad, Helene J., Flydal, Marte I., Mariaule, V., Alvira, S., Cuéllar, J., Haavik, J., Soulé, J., Valpuesta, José M.*, et al.* (2015). Arc is a flexible modular protein capable of reversible self-oligomerization. Biochemical Journal *468*, 145-158.

Nair, R.R., Patil, S., Tiron, A., Kanhema, T., Panja, D., Schiro, L., Parobczak, K., Wilczynski, G., and Bramham, C.R. (2017). Dynamic Arc SUMOylation and Selective Interaction with F-Actin-Binding Protein Drebrin A in LTP Consolidation In Vivo. Frontiers in Synaptic Neuroscience *9*, 8.

Neves, G., Cooke, S.F., and Bliss, T.V.P. (2008). Synaptic plasticity, memory and the hippocampus: a neural network approach to causality. Nat Rev Neurosci *9*, 65-75.

Onyango, I.G., Dennis, J., and Khan, S.M. (2016). Mitochondrial Dysfunction in Alzheimer's Disease and the Rationale for Bioenergetics Based Therapies. Aging and Disease *7*, 201-214.

Palop, J.J., and Mucke, L. (2010). Amyloid-β Induced Neuronal Dysfunction in Alzheimer's Disease: From Synapses toward Neural Networks. Nature neuroscience *13*, 812-818.

Pearson, R.C., Esiri, M.M., Hiorns, R.W., Wilcock, G.K., and Powell, T.P. (1985). Anatomical correlates of the distribution of the pathological changes in the neocortex in Alzheimer disease. Proceedings of the National Academy of Sciences of the United States of America *82*, 4531-4534.

Plath, N., Ohana, O., Dammermann, B., Errington, M.L., Schmitz, D., Gross, C., Mao, X., Engelsberg, A., Mahlke, C., Welzl, H.*, et al.* (2006). Arc/Arg3.1 Is Essential for the Consolidation of Synaptic Plasticity and Memories. Neuron *52*, 437-444.

Prince, M.J., Wimo, A., Guerchet, M.M., Ali, G.C., Wu, Y.-T., and Prina, M. (2015). World Alzheimer Report 2015 - The Global Impact of Dementia (Alzheimer's Disease International).

Purcell, S.M., Moran, J.L., Fromer, M., Ruderfer, D., Solovieff, N., Roussos, P., O'Dushlaine, C., Chambert, K., Bergen, S.E., Kahler, A.*, et al.* (2014). A polygenic burden of rare disruptive mutations in schizophrenia. Nature *506*, 185-190.

Radde, R., Bolmont, T., Kaeser, S.A., Coomaraswamy, J., Lindau, D., Stoltze, L., Calhoun, M.E., Jäggi, F., Wolburg, H., Gengler, S.*, et al.* (2006). Aβ42-driven cerebral amyloidosis in transgenic mice reveals early and robust pathology. EMBO Reports *7*, 940-946.

Rothschild, G., Eban, E., and Frank, L.M. (2017). A cortical-hippocampal-cortical loop of information processing during memory consolidation. Nat Neurosci *20*, 251-259.

Rudinskiy, N., Hawkes, J.M., Betensky, R.A., Eguchi, M., Yamaguchi, S., Spires-Jones, T.L., and Hyman, B.T. (2012). Orchestrated experience-driven Arc responses are disrupted in a mouse model of Alzheimer's disease. Nat Neurosci *15*, 1422-1429.

Scheff, S.W., Price, D.A., Schmitt, F.A., and Mufson, E.J. (2006). Hippocampal synaptic loss in early Alzheimer's disease and mild cognitive impairment. Neurobiology of Aging *27*, 1372-1384.

Selkoe, D.J. (2002). Alzheimer's Disease Is a Synaptic Failure. Science *298*, 789-791.

Selkoe, D.J. (2008). Soluble Oligomers of the Amyloid β-Protein Impair Synaptic Plasticity and Behavior. Behavioural brain research *192*, 106-113.

Selkoe, D.J., and Hardy, J. (2016). The amyloid hypothesis of Alzheimer's disease at 25 years. EMBO molecular medicine *8*, 595-608.

Serrano-Pozo, A., Frosch, M.P., Masliah, E., and Hyman, B.T. (2011). Neuropathological Alterations in Alzheimer Disease. Cold Spring Harbor Perspectives in Medicine: *1*, a006189.

Shankar, G.M., Li, S., Mehta, T.H., Garcia-Munoz, A., Shepardson, N.E., Smith, I., Brett, F.M., Farrell, M.A., Rowan, M.J., Lemere, C.A.*, et al.* (2008). Amyloid-[beta] protein dimers isolated directly from Alzheimer's brains impair synaptic plasticity and memory. Nat Med *14*, 837-842.

Shepherd, J.D., and Bear, M.F. (2011). New views of Arc, a master regulator of synaptic plasticity. Nat Neurosci *14*, 279-284.

Shi, Q., Chowdhury, S., Ma, R., Le, K.X., Hong, S., Caldarone, B.J., Stevens, B., and Lemere, C.A. (2017). Complement C3 deficiency protects against neurodegeneration in aged plaque-rich APP/PS1 mice. Science Translational Medicine *9*.

Smith, A.D. (2002). Imaging the progression of Alzheimer pathology through the brain. Proceedings of the National Academy of Sciences of the United States of America *99*, 4135-4137.

Soule, J., Messaoudi, E., and Bramham, C.R. (2006). Brain-derived neurotrophic factor and control of synaptic consolidation in the adult brain. Biochem Soc Trans *34*, 600-604.

Squire, L.R., Berg, D., Bloom, F.E., Lac, S.d., Ghosh, A., Spitzer, N.C., and Squire, L.R. (2013). Fundamental Neuroscience, Fourth Edi edn (Academic Press).

Squire, L.R., Genzel, L., Wixted, J.T., and Morris, R.G. (2015). Memory Consolidation. Cold Spring Harbor Perspectives in Biology *7*.

Thal, D.R., Rub, U., Orantes, M., and Braak, H. (2002). Phases of A beta-deposition in the human brain and its relevance for the development of AD. Neurology *58*, 1791-1800.

Ulrich, J.D., and Holtzman, D.M. (2016). TREM2 Function in Alzheimer's Disease and Neurodegeneration. ACS chemical neuroscience *7*, 420-427.

Walker, L.C., Diamond, M.I., Duff, K.E., and Hyman, B.T. (2013). Mechanisms of protein seeding in neurodegenerative diseases. JAMA Neurology *70*, 304-310.

Wang, Y., and Mandelkow, E. (2016). Tau in physiology and pathology. Nat Rev Neurosci *17*, 22-35.
Wolfe, M.S. (2006). The γ-Secretase Complex: Membrane-Embedded Proteolytic Ensemble. Biochemistry *45*, 7931-7939.
Wu, J., Petralia, R.S., Kurushima, H., Patel, H., Jung, M.-y., Volk, L., Chowdhury, S., Shepherd, J.D., Dehoff, M., Li, Y.*, et al.* (2011). Arc/Arg3.1 Regulates an Endosomal Pathway Essential for Activity-Dependent β-Amyloid Generation. Cell *147*, 615-628.
Young-Pearse, T.L., Chen, A.C., Chang, R., Marquez, C., and Selkoe, D.J. (2008). Secreted APP regulates the function of full-length APP in neurite outgrowth through interaction with integrin beta1. Neural Development *3*, 15-15.
Zhang, H., Ma, Q., Zhang, Y.-w., and Xu, H. (2012a). Proteolytic processing of Alzheimer's β-amyloid precursor protein. Journal of neurochemistry.
Zhang, H., Ma, Q., Zhang, Y.-w., and Xu, H. (2012b). Proteolytic processing of Alzheimer's β-amyloid precursor protein. Journal of Neurochemistry *120*, 9--21.
Zheng, H., and Koo, E.H. (2006). The amyloid precursor protein: beyond amyloid. Molecular Neurodegeneration *1*, 5-5.

Appendix 1

Co-immunoprecipitation in rat

Arc and several known binding partners were successfully co-immunoprecipitated using the initial protocol (as described in the materials and methods chapter), before optimization for mouse (experiments carried out by Sudarshan Patil) (Figure A1). Samples were hippocampus collected from adult rats, LTP induced in the ipsilateral with HFS. IP of Arc shows co-IP of Drebrin A (Dbn A), Dynamin 2 (Dnm2), and Syntaxin 4 (Stx4) (A). IP of Stx4 shows co-IP of Synaptotagmin 1 (Syt1), Arc, and Stx4 (B). IP of Dnm2 shows co-IP of Arc (C).

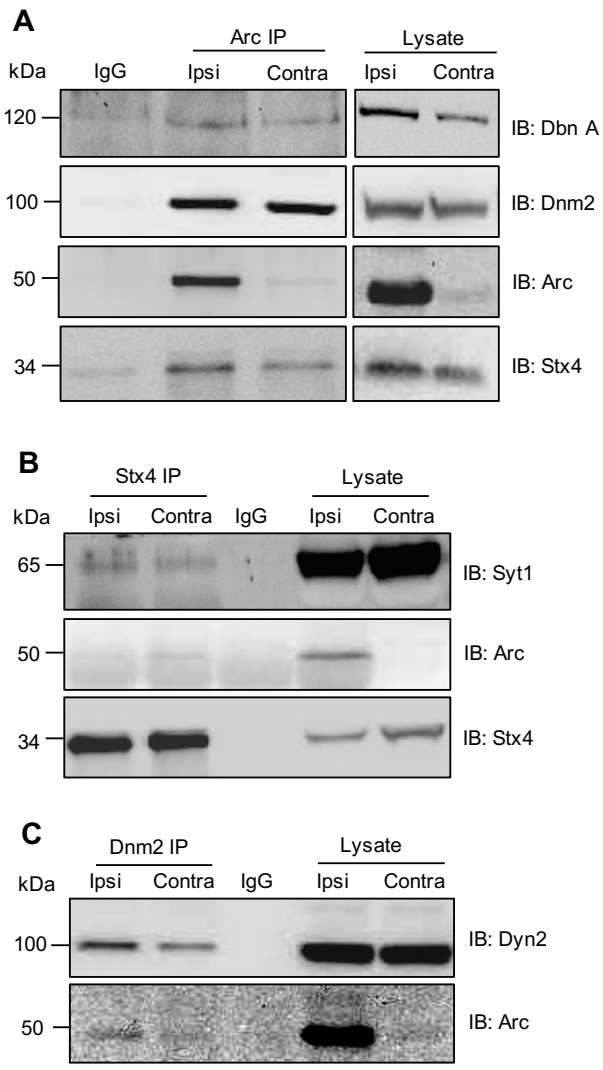

Figure A1 Co-immunoprecipitation of Arc, Stx4, and Dnm2 and respective known binding partners in rat hippocampus (ipsilateral stimulated with HFS) show co-immunoprecipitation of Arc and known binding partners (electrophysiology and co-immunoprecipitations performed by Sudarshan Patil). (A) IP of Arc shows co-IP of Drebrin A (Dbn A), Dynamin 2 (Dnm2), and Syntaxin 4 (Stx4). (B) IP of Stx4 shows co-IP of Synaptotagmin 1 (Syt1), Arc, and Stx4. (C) IP of Dnm2 shows co-IP of Arc.

Appendix 2

Ponceau staining

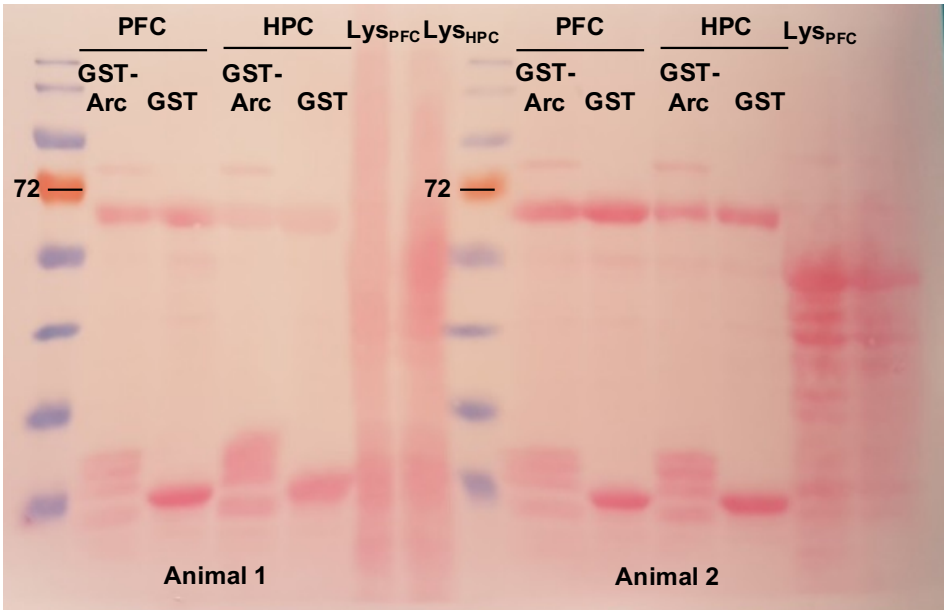

Figure A2 Ponceau staining of membrane after GST-pulldown using lysate from two rats.